



Published in final edited form as:

*Nat Rev Mater.* 2020 January ; 5(1): 20–43. doi:10.1038/s41578-019-0148-6.

## Hydrogel microparticles for biomedical applications

Andrew C. Daly<sup>1,4</sup>, Lindsay Riley<sup>2,4</sup>, Tatiana Segura<sup>2,3,\*</sup>, Jason A. Burdick<sup>1,\*</sup>

<sup>1</sup>Department of Bioengineering, University of Pennsylvania, Philadelphia, PA, USA.

<sup>2</sup>Department of Biomedical Engineering, Duke University, Durham, NC, USA.

<sup>3</sup>Departments of Dermatology and Neurology, Duke University, Durham, NC, USA.

<sup>4</sup>These authors contributed equally: Andrew C. Daly, Lindsay Riley

### Abstract

Hydrogel microparticles (HMPs) are promising for biomedical applications, ranging from the therapeutic delivery of cells and drugs to the production of scaffolds for tissue repair and bioinks for 3D printing. Biologics (cells and drugs) can be encapsulated into HMPs of predefined shapes and sizes using a variety of fabrication techniques (batch emulsion, microfluidics, lithography, electrohydrodynamic (EHD) spraying and mechanical fragmentation). HMPs can be formulated in suspensions to deliver therapeutics, as aggregates of particles (granular hydrogels) to form microporous scaffolds that promote cell infiltration or embedded within a bulk hydrogel to obtain multiscale behaviours. HMP suspensions and granular hydrogels can be injected for minimally invasive delivery of biologics, and they exhibit modular properties when comprised of mixtures of distinct HMP populations. In this Review, we discuss the fabrication techniques that are available for fabricating HMPs, as well as the multiscale behaviours of HMP systems and their functional properties, highlighting their advantages over traditional bulk hydrogels. Furthermore, we discuss applications of HMPs in the fields of cell delivery, drug delivery, scaffold design and biofabrication.

---

Owing to their high water content, diverse properties and similarity to the native extracellular matrix (ECM), hydrogels are used as substrates for cell culture<sup>1</sup>, templates for tissue engineering<sup>2</sup> and vehicles for drug and protein delivery<sup>3</sup>. Traditionally, hydrogels are cross-linked into continuous volumes (bulk hydrogels) with external dimensions at the millimetre scale or larger and a mesh size at the nanometre scale that permits molecule diffusion. A micrometre-scale porosity can be introduced into a bulk hydrogel using various processing techniques, such as porogen leaching<sup>4</sup>, cryogel formation<sup>5</sup> or electrospinning<sup>6</sup>. However, bulk hydrogels are not always suited for their intended applications, particularly in cases in which injection is needed or smaller sizes are required.

---

\* [tatiana.segura@duke.edu](mailto:tatiana.segura@duke.edu); [burdick2@seas.upenn.edu](mailto:burdick2@seas.upenn.edu).

Author contributions

All authors contributed equally to the preparation of this manuscript.

Competing interests

The authors declare no competing interests.

Publisher's note

Springer Nature remains neutral with regard to jurisdictional claims in published maps and institutional affiliations.

As an alternative, various techniques have been developed to fabricate hydrogels as microscale particles (~1–1,000  $\mu\text{m}$ ), called hydrogel microparticles (HMPs) or microgels. HMPs can be made from both natural and synthetic polymers, and can be fabricated into a variety of shapes and sizes using techniques that are often compatible with the encapsulation of biologics (for example, cells and drugs). Whereas the dynamics of polymers in solution, such as prior to hydrogel formation, are driven by thermal fluctuations, the larger HMPs are dominated by gravity, which allows for particle settling. HMPs can be utilized as distinct units or in aggregation; thus, we classify HMP systems into three categories: HMP suspensions, granular hydrogels and HMP composites (FIG. 1). In HMP suspensions, the HMPs reside in a fluid (liquid or air), with minimal interactions between particles. When the particle-packing density is increased and the particle-particle interactions that govern bulk assembly properties arise, HMPs form granular hydrogels. Granular hydrogels primarily exist in a jammed state, where they can range from a loose-packing configuration with high porosity to an ultraclose-packing state in which HMPs deform and the interstitial space collapses, resulting in a loss of microporosity. Finally, HMP composites are obtained when HMPs are embedded within a bulk hydrogel.

HMPs have a number of unique properties compared to bulk hydrogels that make them attractive for biomedical applications. First, their small size enables injection through small needles and catheters and inhalation of particles, which is advantageous for minimally invasive delivery of cells and biologics. The physical interactions between particles in granular systems often lead to a shear-thinning behaviour that permits injection and then a solid-like consistency after injection without the need for chemical modification<sup>7</sup>; however, interparticle cross-linking chemistries may also be incorporated to further alter the granular hydrogel properties<sup>8</sup>. Second, HMP systems are inherently modular, as multiple HMP populations with varying composition, size and contents can be mixed to create diverse materials<sup>9</sup>. Third, granular hydrogels can possess significant porosity (or void space) owing to the interstitial space between HMPs. The level of porosity scales with the size and packing density of HMPs and can be tuned to support cell proliferation and migration<sup>10</sup>.

In this Review, we discuss advances in the development of HMPs for biomedical applications. First, we introduce and compare methods used to fabricate HMPs, including batch and microfluidic emulsions, lithography, spraying and mechanical fragmentation. Then, we discuss the multiscale properties of HMP systems, including mechanical properties, injectability and porosity. Finally, we survey recent applications of HMP systems in cell delivery, drug delivery, scaffold building and biofabrication. The overall goal of this Review is to introduce the biomedical potential of these materials, as well as provide guidance for methods to fabricate and characterize them.

## Fabrication of HMPs

A variety of fabrication techniques can be used to fabricate HMPs across various hydrogel types and cross-linking methods (FIG. 2). We can categorize them as batch emulsions, microfluidic emulsions, lithography, EHD spraying and mechanical fragmentation. In general, these approaches include the formation of droplets of hydrogel precursors that are

then cured into HMPs, the spatial control of light to cure HMPs from hydrogel precursor solutions or the disruption of bulk hydrogels into HMPs.

Approaches such as batch emulsions and mechanical fragmentation are popular because of their simplicity and the speed at which HMPs can be produced. However, more advanced strategies, such as microfluidic emulsions, lithography and EHD spraying, offer improved control over the formation of individual particles and have enabled the production of more monodisperse HMPs with variations in internal and external architectures. Key process parameters such as the rate of particle production and the particle size distribution can vary significantly across fabrication techniques: we outline these parameters in TABLE 1.

Each fabrication technique imposes constraints on the hydrogels that can be processed. For example, the rheological behaviour and cross-linking mechanism of the hydrogel must be compatible with the chosen method. Thus, the fabrication technique should be selected based on its compatibility with the selected hydrogel, as well as on the desired HMP properties (such as size and dispersity) and access to specialized equipment (microfluidic emulsion, lithography and EHD spraying require more advanced equipment, whereas batch emulsions and fragmentation require relatively simple equipment). In this section, we discuss the strengths, limitations and compatibility with cell and drug encapsulation of each technique. We also highlight the hydrogel chemistry and cross-linking methods used in each fabrication approach, which are summarized in TABLE 2.

### Batch-emulsion techniques

Emulsion techniques use immiscible oil and aqueous hydrogel precursor solutions to generate droplets that can then be cross-linked into HMPs. In a batch process, an aqueous precursor solution containing the hydrogel prepolymer and an initiator and/or cross-linker is combined with the oil in a single container, potentially with a surfactant to stabilize the emulsion. Mechanical mixing is used to homogenize the solution and generate aqueous droplets surrounded by an oil phase (FIG. 2a). The extent and timing of mixing can influence the size and dispersity of the resulting droplets. The droplets are then cross-linked and the oil phase is removed using a series of washing, centrifugation and filtration steps. Several hydrogel cross-linking approaches are compatible with batch-emulsion techniques (TABLE 2). Photocross-linking is commonly used because external light sources induce cross-linking while the droplets of precursor solutions are suspended in the oil phase. For example, acrylated or methacrylated poly(ethylene glycol) (PEG) HMPs can be photocross-linked using radical polymerizations if a suitable initiator is included in the aqueous phase<sup>11</sup>. Alternatively, changes in temperature (cooling) can be used to cross-link thermosensitive hydrogels such as gelatin<sup>12</sup>.

The main advantages of batch-emulsion methods are their simplicity and the high particle-production rates, which are only limited by the container volume and by the ability to mix the emulsion. These methods are also compatible with biologics such as small molecules and growth factors, which can be simply dissolved in the hydrogel precursor solutions before the formation of the emulsion<sup>13</sup>. Batch-emulsion techniques have also been successfully used to encapsulate cells within HMPs through suspension in the aqueous solution prior to emulsification<sup>11,12</sup>.

One of the main limitations of batch emulsions is the polydispersity of the resulting HMPs, as there is limited control over the formation of individual particles<sup>14</sup>. This may also lead to batch-to-batch variations if the mixing procedures are not performed identically each time. The importance of polydispersity depends on the application: for example, when HMPs are used to release growth factors, diffusion may depend on their polydispersity and on particle sizes. It has been demonstrated that HMP populations with comparable mean diameters but prepared with either batch or microfluidic emulsions possess distinct release profiles, with greater variability in the population prepared by batch emulsion, which displays an earlier burst release of the encapsulated drug<sup>14</sup>. Further, HMP polydispersity makes it challenging to control the number of cells contained within each HMP; however, polydisperse HMP suspensions can be serially filtered with increasingly smaller filters to achieve a more monodisperse suspension<sup>15</sup>. If the batch-emulsion process is performed in a repeatable manner and its influence on HMP properties is understood, the drawbacks related to polydispersity can be minimal.

Although this method is used less frequently, HMPs can also be produced using all-aqueous, two-phase separation techniques<sup>16</sup>. Early work in this area leveraged phase-separation phenomena that occur through simple mixing of aqueous solutions of PEG and methacrylated dextran and subsequent cross-linking with light after separation<sup>17</sup>. PEG can also be used to form HMPs, exploiting phase separation above a lower critical solution temperature, including across a range of sizes with control over the thermodynamics and kinetics of the phase-separation process<sup>18</sup>. For example, HMPs were formed from reactive PEG derivatives that underwent thermally induced phase separation, and their size was dependent on the kinetics of gelation, influenced by temperature and pH<sup>19</sup>. Gelatin-based HMPs have also been fabricated with two-phase separation techniques exploiting the formation of simple coacervates in the presence of polyanions such as alginate under low-pH conditions<sup>20</sup>. For example, spontaneous HMP formation was observed following mixing of oxidized and methacrylated alginate and gelatin methacrylamide (GelMA) in aqueous solutions at low pH, resulting in a composite hydrogel system containing growth-factor-loaded GelMA compartments surrounded by an alginate bulk phase<sup>20</sup>.

### Microfluidic-emulsion techniques

The limitations of batch-emulsion protocols motivated seminal studies in the early 2000s that demonstrated the potential of more controlled emulsions in HMP fabrication, such as in flow-focusing microfluidic devices<sup>21,22</sup>. Controlled droplet formation can be achieved by directing the flow of oils and aqueous solutions at intersection points, where shear forces and hydrophobic interactions induce the formation of aqueous droplets within an oil phase (FIG. 2b). Importantly, by varying the geometry of the intersection and the relative flow rates between the two phases, it is possible to control the droplet diameter, which is in the micrometre range (5–500  $\mu\text{m}$ )<sup>23,24</sup>. In addition, if the flow rates are maintained, monodisperse particle populations with dispersity indexes as low as 1–2% can be produced<sup>25,26</sup>. As a result, microfluidic technology has been widely adopted to produce HMPs across a wide variety of hydrogels<sup>8,23,27</sup> (TABLE 2). Microfluidic emulsions are also compatible with small-molecule or protein encapsulation; the improved size distribution offers greater control over subsequent release profiles<sup>13,14,28–30</sup>. In addition, by

incorporating cells in the aqueous phase at a defined concentration, it is possible to predict and control the number of cells encapsulated in single HMPs<sup>31–33</sup>.

Microfluidic methods impose two main requirements on the hydrogel precursor solution. First, the solution must have a relatively low viscosity, so that it can be pumped through narrow microchannels at low pressures. Second, the droplets must cross-link rapidly during collection to prevent droplet coalescence. Many cross-linking strategies have been introduced in which droplets are cross-linked either ‘on-chip’ or ‘off-chip’; on-chip approaches are preferred because they limit droplet coalescence. Photocross-linking has been used with macromers such as polyethylene (glycol) diacrylate (PEGDA) and GelMA because they can be rapidly cross-linked using externally applied light<sup>34,35</sup>. Photoinitiated thiol-ene cross-linking has also been used to process HMPs, for example with norbornene-modified hyaluronic-acid and PEG macromers, which were cross-linked in the presence of dithiol cross-linkers and radical initiators<sup>7,36</sup>. Thermoresponsive hydrogels such as agarose can also be processed into HMPs by cooling the droplets during collection<sup>7,37</sup>.

Gelation of the hydrogel precursor can also be achieved through mixing or introduction of reactive components on-chip. Cross-linkers or initiators can be added to the oil phase, which subsequently diffuses into the aqueous phase to initiate cross-linking. For example, PEG maleimide HMPs have been fabricated by incorporating dithiol cross-linkers into the oil phase, where they can diffuse into the droplets to induce a Michael-addition reaction<sup>38</sup>. Advanced microfluidic devices can also be used to mix reactive components, for example using multiple flow-focusing junctions. The mixed aqueous phase can then be rapidly focused at a second emulsion junction for droplet formation and cross-linking over time. Using this approach, HMPs have been fabricated through a Michael-addition reaction between PEG thiol and PEG vinyl sulfone<sup>39</sup>. In a similar approach, degradable HMPs were formed through a reaction between cysteine-terminated, degradable matrix metalloproteinase (MMP)-sensitive cross-linkers and PEG vinyl sulfone<sup>8</sup>.

The main advantage of microfluidic approaches is the good control over the droplet-formation process, which can be precisely engineered by both designing microfluidic channels with specified geometries and controlling inputs such as flow rates. Typically, microfluidic junctions are made using microfabricated polydimethylsiloxane (PDMS) moulds that can be engineered to user-defined dimensions using soft lithography or 3D printing. Capillary-based microfluidic devices, in which glass capillaries are coaxially aligned in either co-flow or flow-focusing configurations, can also be used to generate microfluidic emulsions. A range of microfluidic techniques for generating compartmentalized HMPs have been developed<sup>40–42</sup>. For example, Janus HMPs were obtained by directing two aqueous solutions at a primary junction with laminar flow and then breaking them into droplets by further flow focusing at a secondary emulsion junction<sup>43</sup> (FIG. 3a). Glass microcapillary devices can be used to form double emulsions, where particles of various internal complexities can be made, dependent upon the relative flow rates between the outer, middle and inner fluids<sup>25</sup> (FIG. 3b). This high level of control over the droplet-formation process has enabled the formation of HMPs with either multiple drug-loaded compartments, where the drug-release rate from a particular compartment can be independently tuned by varying the hydrogel properties of that compartment and the overall

release is based on the total release over time from all compartments<sup>44,45</sup>, or with structured co-cultures of cells<sup>46,47</sup>. A promising alternative is the design of centrifuge-based microfluidic devices to produce compartmental microparticles without oil, with the particle size controlled by the capillary diameter and centrifugal force<sup>48</sup>.

As an alternative to chip-based microfluidics, in-air microfluidic methods have been developed. In these methods, two microscale liquid streams are jetted together and forced to collide, leading to droplet formation<sup>49,50</sup>. Compared to microchannel-based on-chip techniques, higher liquid-flow rates can be achieved, which leads to faster particle-production rates (10–100 times faster). In addition, when reactive liquids are jetted towards each other (for example, alginate and calcium chloride), the HMPs can be directly deposited into 3D constructs. There is great potential in techniques such as these, which need to be further explored to exploit their advantages over other emulsion-based methods.

The major limitation of microfluidic approaches is that they are relatively low throughput compared to batch emulsions. This issue becomes exacerbated when attempting to produce smaller-diameter HMPs because the volumetric throughput decreases with the cube of the droplet diameter. However, higher throughput rates can be achieved using parallelized microfluidic devices containing multiple junctions on a single device<sup>51–54</sup>. To ensure that monodisperse particle populations are produced when using parallelized devices, the channel geometry must be designed to accommodate pressure drops and flow fluctuations throughout the device. For example, the successful encapsulation of viable cells within monodisperse PEG HMPs was demonstrated using a parallelized, double-layer PDMS device with a throughput six times higher than that of single-channel devices<sup>33</sup>. Microfluidic devices also classically produce spherical particles as a product of the surface-tension-driven droplet formation and alternative techniques may be needed if non-spherical particle geometries are desired.

## Lithography

HMPs can also be produced using lithographic methods, in which photopolymerization is used to template hydrogels at the microscale. There are three main classes of lithography technologies: imprint lithography, photolithography and flow lithography<sup>55</sup> (FIG. 2c). In imprint lithography, a hydrogel precursor is loaded into a templated mould with the negative features of the desired HMPs for cross-linking and then cured. Photolithography uses templated photomasks to selectively cure regions of a hydrogel precursor to form HMPs. Lastly, flow lithography uses a photomask to cure regions of a flowing hydrogel precursor solution at regular intervals to form HMPs. The main advantage of lithography technologies is that the geometrical features of the mask or mould can be tightly controlled, resulting in great control over the geometry and monodispersity of the HMPs<sup>56–58</sup>. In addition, lithographic approaches are widely compatible with cell encapsulation and no oil or surfactants are required to induce particle formation<sup>34,59</sup>.

Advances in microfabrication techniques have enabled the production of moulds and masks with features defined at the nanometre scale, making it possible to generate designer HMPs with tailored internal and external architectures that could not be achieved with other fabrication methods<sup>56–58,60–62</sup>. However, there are several constraints on the HMP



geometries that can be obtained. Imprint-lithography approaches present the practical constraint of needing to remove the cross-linked HMPs from the mould, which limits the complexity of the achievable internal or external features. With photolithography, only relatively simple geometries such as cubes, cuboids, discs, bars and stars can be obtained<sup>55,61</sup>. To enable the production of HMPs with complex 3D geometries, multiphoton light sources have to be used<sup>63,64</sup>. Advanced lithographic assemblies that facilitate sequentially layered polymerization to produce complex 3D HMPs have also been developed<sup>56</sup> (FIG. 3c).

A range of photocross-linking chemistries have been explored to produce HMPs using lithography (TABLE 2). The most commonly used hydrogels are acrylated or methacrylated PEGs, which are simple, tunable and biocompatible<sup>59,65,66</sup>. For example, PEGDA and poly(ethylene glycol) dimethacrylate (PEGMA) hydrogels can be cross-linked in seconds through photoinduced radical polymerization in the presence of a photoinitiator. Naturally derived hydrogels such as hyaluronic acid and gelatin can also be functionalized with reactive groups that make them processable by lithography<sup>58,67</sup>. Thiol-ene-based, step-growth photocross-linking approaches have been used to generate HMPs using modified poly(vinyl alcohol) (PVA)<sup>68</sup> or hyaluronic acid vinyl ester with two-photon photolithography<sup>69</sup>.

A major challenge with lithography approaches is that they are relatively low throughput compared to other methods. Specifically, the particle-production rate is limited by the size of the moulds or masks that can be prepared using available microfabrication techniques and by the field of view of the light source or objective. Fast hydrogel curing times are generally preferred because they increase particle-production rates. For example, by increasing the number of functional groups on the macromer (for example, acrylate or norbornene) or the macromer concentration, the rate of polymerization and the final mechanical properties increased<sup>70–72</sup>. Further, increasing the light-source intensity or the initiator concentration (for example, I2959 for ultraviolet light and lithium phenyl-2,4,6-trimethylbenzoylphosphinate (LAP) for visible light) reduces the curing time required to reach a desired cross-linking density<sup>73,74</sup>. Flow-lithography techniques offer the greatest throughput because they can be integrated with microfluidic techniques<sup>61,65</sup> and parallelized<sup>75</sup>. A method that is not widely adopted but has good performance is the particle replication in non-wetting templates (PRINT) system, which can produce HMPs with controlled sizes and shapes in a high-throughput manner through integration with a roll-to-roll manufacturing process that facilitates scalable particle-production rates<sup>62,66</sup>.

### Electrohydrodynamic-spraying methods

EHD-spraying methods are less commonly used than the techniques discussed so far. During EHD spraying, a hydrogel precursor solution is extruded through a syringe while a voltage is applied at the needle tip. Beyond a critical threshold, the applied voltage overcomes the surface tension at the needle tip, leading to the formation of a charged jet of droplets that are attracted towards a collecting substrate<sup>76</sup> (FIG. 2d). The droplets are then cross-linked in the collecting bath, and their size depends on parameters such as the applied voltage, needle diameter and polymer flow rate<sup>77</sup>, and can be as small as 1  $\mu\text{m}$ <sup>78</sup>. However, achieving

monodisperse particle populations is challenging, and dispersity indexes higher than 5% are often reported<sup>79,80</sup>. Alginate is widely used for EHD spraying because it can be directly sprayed into a calcium-chloride solution to induce immediate cross-linking of the droplets<sup>76,77,81</sup>. Chitosan HMPs have been processed by spraying into a tripolyphosphate solution to cross-link via electrostatic interactions<sup>82</sup>. Photocross-linkable hydrogels have been processed by spraying into a bath that is simultaneously exposed to light<sup>79,80</sup>. Finally, this technique is compatible with cell encapsulation<sup>76,77,83,84</sup>. Similar to emulsion approaches, the polydisperse particles can be passed through filters to achieve a more monodisperse population.

### Mechanical-fragmentation methods

In mechanical-fragmentation methods, HMPs are produced by mechanically breaking a preformed bulk hydrogel into microscale particles (FIG. 2e). For example, a cross-linked hydrogel can be mechanically forced through a fine steel mesh to form smaller particles. The size of the HMPs can then be controlled through the pore size of the mesh. HMPs with diameters of 15–30  $\mu\text{m}$  have been obtained this way<sup>85</sup>. Another simple fragmentation method involves breaking a cross-linked hydrogel into particles using a simple rotational blender. This method has been used to generate blended gelatin slurries composed of microparticles with diameters of 120–300  $\mu\text{m}$ <sup>86</sup>. The main advantages of microparticulation approaches are their speed and simplicity, which make it possible to rapidly generate large volumes of microparticles in a single process. However, a major limitation is that there is little control over the formation of individual particles, which results in polydisperse size distributions. It is also not clear whether these approaches are compatible with cell encapsulation, and, to the best of our knowledge, no studies on this aspect are available in the literature.

### Properties of HMP systems

The physical properties of HMP systems are multiscale and depend on the properties of the individual HMPs, on their packing density and on the properties of the continuous phase. HMP suspensions, granular hydrogels and HMP composites each possess unique functional properties not present in bulk hydrogels. For example, HMP suspensions can be easily delivered through small needles or inhalers for minimally invasive delivery of cells and biologics. Granular hydrogels (FIG. 4) form particle scaffolds that open up new building approaches, including microporosity (owing to the interstitial space among HMPs) and scaffold modularity (owing to the mixing of multiple HMP populations)<sup>87</sup>. Granular hydrogels also display a shear-thinning behaviour that can be exploited for injectability and 3D printing applications<sup>9</sup>. In this section, we describe the different classes of HMP systems, with particular focus on their macroscale and microscale mechanics, porosity and diffusivity. We then describe some of the unique functional features of HMPs (injectability, heterogeneity and porosity) relevant for biomedical applications.

### Multiscale properties of HMP systems

**HMP suspensions.**—HMP suspensions comprise dilute HMPs in a fluid, such as liquid or air (FIG. 1). The macroscale mechanical and rheological behaviours of HMP suspensions



are largely governed by the properties of the continuous phase because interparticle interactions are negligible. The individual mechanical properties of the HMPs within the system depend on the polymer type and density, as well as the extent of cross-linking between polymer chains. Due to the relatively low packing density of HMPs in suspensions, the overall system diffusivity is high; however, diffusivity within an individual HMP is governed by the polymer mesh size. The concept of microporosity does not apply to HMP suspensions because microporosity is defined in the context of a solid-like material, but the particle-packing density is too low in these systems. Larger and denser microparticles (usually larger than 10  $\mu\text{m}$  in diameter) are less sensitive to thermal forces that lead to Brownian motion and more affected by gravitational forces. This, in conjunction with interparticle friction, promotes HMP settling and packing<sup>88–90</sup>. Therefore, under static, non-mixing, non-flow conditions, suspensions of HMPs greater than 10  $\mu\text{m}$  readily settle into a jammed state and transition to a granular hydrogel. HMP suspensions are generally used for cell or drug delivery, when interactions between particles are not needed to achieve effective therapeutic outcomes.

**Granular hydrogels.**—Granular hydrogels (FIG. 4) comprise an agglomeration of HMPs in the jammed state, where the term ‘jammed’ implies that an inside particle can only move if its neighbouring particles also move<sup>91</sup>. Generally, granular materials are composed of solid particles that readily sediment and experience frictional forces between touching particles<sup>88,90</sup>. Interparticle friction among HMPs in granular hydrogels is attributed to polymer interactions on the surface of HMPs; the amount of friction is influenced by the polymer type, microparticle chemistry and properties of the continuous phase of the material (such as viscosity and polymer-solvent interactions)<sup>92</sup>. As the HMP-packing density reaches that of the jammed state, interparticle friction aids in the transition from a liquid-like to a solid-like state<sup>88</sup>. Looking at the properties of granular hydrogels across various length scales, the polymer network is important at the nanoscale and it can influence the properties of individual HMPs at the microscale and those of the granular hydrogel at the millimetre scale (FIG. 4a).

The jamming transition occurs when the particle-packing density (or particle-volume fraction,  $\phi$ ) is sufficiently high and under appropriate conditions of stress and temperature<sup>87,90</sup>. Reducing the continuous phase of the material can promote HMP packing towards the jammed state<sup>7</sup>. The resulting jammed system behaves as a solid-like mass of touching particles; the precise particle-packing density largely influences hydrogel dynamics. Classically, hard-sphere packing is categorized into three general ranges: random loose packing ( $\phi > 0.58$ ), random close packing ( $0.58 < \phi < 0.64$ ) and maximally jammed, perfect packing ( $\phi \approx 0.74$ ). At  $\phi \approx 0.58$ , particles are minimally jammed but configurationally stable. At  $\phi \approx 0.64$ , particles are maximally jammed in a random configuration in which additional jamming would require particle deformation<sup>90,93</sup>. Thus, granular hydrogels of spherical HMPs theoretically lie within a range of  $\phi \approx [0.58–0.64]$ . In reality, however, HMP systems are much more complex, owing to HMP deformability, interparticle friction and non-spherical, non-uniform HMP shapes, all of which may allow for states with  $\phi > 0.74$  (REF<sup>94</sup>). External forces such as centripetal forces or compression can be used to reach a state of ultraclose packing ( $\phi \approx 1$ ), in which the interstitial space begins

to collapse and flat-faced facets form between touching, deformed HMPs (FIG. 4b). To understand these behaviours, numerical simulations have been used to study the packing of particles of heterogeneous shapes, sizes and deformability<sup>93,95,96</sup>.

Granular hydrogels can swell and compress more than bulk hydrogels, owing to their two-scale matrix structure: intraparticle polymer cross-linking makes up individual HMPs, whereas an interparticle microporous matrix is formed when particles are packed together. The intraparticle matrix is nearly identical to that of a bulk hydrogel, but the microporous scaffold is specific to the jammed state, in which touching particles form the interconnected secondary matrix. This two-scale structure results in a two-phase response to swelling and osmotic compression. Bulk hydrogels can only swell up to the capacity of their polymer matrix, whereas granular hydrogels comprising fully swollen HMPs may continue to swell into the interstitial space of the packed particles until particles begin to pull apart (transitioning towards an HMP suspension)<sup>92</sup>. By contrast, osmotic forces can make HMP suspensions transition to a granular hydrogel phase. Once the jammed state is reached, further compression past a critical force will expel solvent from the decreasing interstitial space until the granular hydrogel begins to behave as a solid bulk gel. Such phenomena are sensitive to HMP stiffness but not to HMP size<sup>92</sup>.

The particulate nature of granular hydrogels makes them respond differently than bulk hydrogels to uniaxial compression, indentation and shear tests. Viscoelastic materials such as bulk hydrogels fracture under an applied force surpassing the yield stress. Granular hydrogels behave in a similar way under exceedingly high compression, when particles are densely packed and deformed. However, below this critical threshold, local slipping and sliding of HMPs helps to accommodate the imposed stress<sup>89,92</sup>. Unlike homogeneous bulk hydrogels, granular hydrogels contain load-bearing force chains, which are paths of touching particles through which stress is transmitted; these chains govern the stability and flowability of the system. Over the range of strains at which granular hydrogels exhibit elastic behaviour, force-chain networks remain constant. However, in the plastic regime, force chains become dynamic and respond to changes in the external load to maintain stable stress states<sup>89,97</sup>. The surface area of the applied load dramatically influences the mechanical response of a granular system: a large surface-area compression may result in minimal HMP displacement, whereas a focused indentation can penetrate the scaffold without fracture by causing local particle displacement. Shear loading of granular hydrogels results in a higher loss modulus (viscous response) under low shear rates than in bulk hydrogels.

Many materials properties influence the mechanical response of granular hydrogels, including polymer type, HMP stiffness, HMP density, HMP charge and interparticle friction. Incorporating a heterogeneous population of HMPs can introduce other interparticle forces that contribute to the dynamics of granular gels, including electrostatic interactions and hydrophobic-hydrophilic interactions. Granular hydrogels that comprise heterogeneous particle sizes may contain ‘rattlers’ or ‘floaters’ (smaller particles that freely traverse the interstitial space of the scaffold)<sup>91,95</sup>; however, these should not significantly impact the jamming properties of the system. When an external force is applied to a granular hydrogel, interparticle friction reduces HMP rearrangement<sup>92</sup>. To fully immobilize particles and fix the packing configuration of a scaffold, HMPs may be cross-linked together to create what is

referred to as a microporous annealed particle (MAP) scaffold<sup>8</sup>. Annealing between HMPs can be achieved using a number of covalent or non-covalent techniques. The mechanical properties of MAP scaffolds are different from those of non-annealed HMP systems<sup>10</sup>, and, although both systems behave as solids under low shear stress, non-annealed HMP systems flow under high shear stress. By contrast, MAP scaffolds reach a higher modulus and do not behave as a liquid at high shear stress unless the annealing chemistry is reversible or non-covalent. Note that MAP scaffolds do not match the mechanical properties of bulk hydrogels with a matching formulation, owing to the lower number of HMP contact points relative to polymer entanglement in a bulk network<sup>15,98</sup>. Material degradation kinetics can also be modulated by HMP annealing, which introduces a tunable degradation parameter that does not exactly mirror the properties of the non-porous matrix composing the HMPs. Additionally, by limiting HMP rearrangement, the void space microarchitecture of the scaffold becomes fixed, offering a more controllable infrastructure.

**HMP composites.**—In HMP composites, the particles are incorporated in a secondary material (such as a hydrogel) (FiG. 1). The mechanical properties of the secondary material typically dominate the behaviour of composite systems, unless the concentration of HMPs is substantial and depending on their size and density. Embedding HMPs in a hydrogel helps to stabilize individual HMPs: the hydrogel acts as a cement to hold HMPs together and can potentially introduce desirable chemical or molecular interactions. HMP composites can also be used to fabricate microporous bulk hydrogels by using the HMPs as a sacrificial porogen that is then washed out (for example, gelatin through heating and cooling steps) after cross-linking the bulk hydrogel phase<sup>99,100</sup>. The dual material inherent to HMP composites can also be exploited for a more complex mechanical behaviour. For example, HMP composites have been used to engineer mechanically tough hydrogels in which the dispersed microgel phase blunts crack propagation under load<sup>101</sup>. HMP composites can also be used to decouple the mechanical and biological properties of a hydrogel. For example, rather than simply increasing the cross-linking density of a hydrogel to make it tougher, which may influence cell behaviour, adding HMPs (such as stiff gellan-gum microgels) to a soft hydrogel was shown to increase its toughness<sup>102</sup>.

### Functional properties of HMP systems

**Injectability.**—A noteworthy feature of HMP systems is that they can be injected using a syringe or catheter (FiG. 4). Preformed bulk hydrogels are challenging to deliver using minimally invasive techniques and must, instead, be shaped and implanted, often involving surgical incisions. Bulk hydrogels are normally only injectable as a homogeneous precursor solution that exhibits liquid-like (viscous) rheological properties until gelation is induced using in situ cross-linking approaches or through the incorporation of shear-thinning cross-links. By contrast, unannealed HMP systems are easily injectable due to their particulate nature and small particle size. Frictional, non-covalent and electrostatic forces among neighbouring HMPs affect their injectability and become increasingly influential as particle packing increases. For example, jammed granular hydrogels exhibit shear-thinning behaviour; thus, large injection forces allow HMPs to collectively flow as a fluid and, once the applied force is attenuated, the HMPs return to a viscoelastic solid state with gel-like rheological properties<sup>7</sup>. Gel stiffness may be further enhanced by annealing HMPs post

injection<sup>8</sup>. The injectability of HMPs has been exploited for several applications, including wound healing and bioprinting, using a wide range of hydrogels. For example, modified hyaluronic-acid HMPs (made using microfluidics) were injected into ischaemic sites within cardiac<sup>9</sup> and brain<sup>103</sup> tissue in rats and mice, respectively, to promote wound healing in a minimally invasive way.

Particle jamming, which regularly occurs under syringe pressure, minimizes turbulent flow and allows HMPs to move as a plug during injection<sup>54,104</sup> (FIG. 4c). When injected into a cavity, HMPs at appropriate packing fractions readily fill the space and take the shape of the cavity, similar to a precursor hydrogel solution; however, the viscoelasticity of particulate hydrogels minimizes their dispersion upon injection<sup>8,103</sup>. Note that unannealed, jammed HMPs behave as a solid unit when injected into tissues that experience low pressure, such as the skin; however, injection into pressurized, confined spaces, such as fluid-filled stroke cavities, may require post-injection HMP annealing to avoid backflow after the syringe is removed<sup>103</sup>. Annealing after injection into highly motile tissues, such as cardiac tissues, may also help to minimize particle dislodging<sup>9</sup> but, depending on the formulation, is not always needed<sup>105</sup>.

**Heterogeneity.**—Incorporating intraparticle and/or interparticle heterogeneity introduces additional complexity to HMP systems that may elicit multifactorial effects at the particle or system level (FIG. 4c). Intraparticle heterogeneity may involve compartmentalizing individual HMPs, altering surface chemistries post production, layering individual HMPs or varying porosity within individual HMPs. Regarding interparticle heterogeneity, HMP species can differ from one another in a multitude of ways, including hydrogel formulation or cargo type. A heterogeneous material can be produced by simply mixing multiple HMP populations until particles are uniformly distributed. Macroscale anisotropy can be achieved by exploiting HMP jamming, which minimizes HMP mixing and allows for physical separation of different HMP agglomerations<sup>104</sup>. To demonstrate the potential complexity of HMP systems, consider a collection of spherical (100- $\mu\text{m}$ ) HMPs in an aqueous medium. In the jammed state, there are roughly 1,000 HMPs per  $\mu\text{L}$  of material. Scaling up, 1 mL of material would contain 1 million distinct HMPs. Thus, there is substantial room for incorporating HMP heterogeneity across various HMP systems.

**Void space and porosity.**—The interstitial space (or void space) among packed HMPs is referred to as the pores of the granular scaffold, and the size of the pores is proportional to the size of the HMPs. Thus, packed HMPs produce micrometre-sized pockets of interstitial space<sup>87</sup>. Cells with diameters on this length scale can, therefore, easily infiltrate and traverse a granular scaffold without needing to degrade the hydrogel, whereas degradation is often needed for cells to infiltrate a bulk hydrogel. Relative to non-porous hydrogels, the microporosity of granular hydrogels increases fluid-flow, mass-transport, permeability and cell-infiltration rates. The system can also accommodate other large entities, such as ECM proteins (which often exceed 200 kDa in size). A reduction in scaffold porosity generally correlates with a reduction in mass-transport rates. The average pore size of a scaffold is affected by HMP shapes and sizes, packing density and stiffness<sup>8,106</sup>. Depending on the degree of HMP jamming and softness, the application of a large external force may result in

the collapse of the interstitial space, so that flat-faced facets form between touching, deformed particles<sup>94</sup> (ultra-close packing in FIG. 4c).

## Applications of HMPs

The properties of HMPs make them promising for numerous biomedical applications, several of which are covered in this section, including cell delivery, drug delivery, scaffold building and biofabrication. The ability to extrude HMP-based biomaterials from syringes or catheters is particularly important for their delivery to tissues. HMPs can be delivered, for example, by intraarticular injection or direct injection into tissues: the modes of delivery of HMPs to various tissues are summarized in FIG. 5.

### HMPs for cell delivery

The delivery of cells to damaged and diseased tissues holds tremendous potential for numerous applications; however, challenges — including limited cell survival and difficult engraftment of transplanted cells following delivery — has hampered progress in this area. This has led to increased interest in the use of delivery vehicles to enhance the integration, viability and function of injected cells<sup>107</sup>. Hydrogels emerged as a platform to increase the localization of cells at the target site following injection and to provide appropriate biophysical and biochemical cues to promote cellular integration and desired function<sup>108–111</sup>. The high water content and tunable properties of hydrogels further motivated their use in this area. Although significant progress has been made, challenges still remain; for example, the large diffusion lengths in bulk hydrogels may limit the oxygen and nutrients that reach transplanted cells. Further, the limited porosity and lack of injectability of many bulk hydrogels impede their use in several applications. These limitations have stimulated interest in the use of HMP systems for cell delivery. In this section, we describe concepts and advances in the use of HMPs for cell delivery and highlight some successful applications.

**Cell encapsulation within HMPs.**—As discussed, a range of HMP fabrication techniques are compatible with cell encapsulation (batch emulsion, microfluidic emulsion, lithography and EHD spraying). Microfluidic emulsions and lithography are often used due to the improved control over particle size and shape that they offer. By controlling process parameters such as the particle size and density of cells within the precursor solution, it is possible to precisely control the number of cells per HMP, down to the single-cell level<sup>33,112</sup>. In addition, by parallelizing channels, it is possible to generate cell-laden HMPs in a high-throughput manner<sup>33,75</sup>.

Cell encapsulation within HMPs offers several advantages compared to encapsulation within bulk hydrogels. A significant challenge with hydrogel-based cell encapsulation is the limited nutrient diffusion within core regions, which is exacerbated as the hydrogel size is increased to clinically relevant dimensions. A common approach to address this problem is the incorporation of nutrient microchannels into the hydrogel<sup>113–116</sup>; however, this can be technically challenging when an injectable material is desired. Packed HMP systems provide an alternative because the microporous interstitial space surrounding the particles enables diffusion. Additionally, granular scaffolds enhance vascularization when compared to bulk

hydrogels in a variety of in vivo environments, which supports the engineering of thicker tissues<sup>8,103</sup>.

When considering the design of HMP cell-encapsulation techniques, it is important to consider both the process that is used to encapsulate the cells (in terms of achieving high viability) and the environment in which the cells are embedded (in terms of enabling function). The importance of the cellular microenvironment on cell function has emerged over the past decades: features such as the mechanics of the environment may change cellular mechanosensing, and the incorporation of ligands may enable cell adhesion<sup>1,117</sup>; thus, there is now a focus on these features when designing HMP environments. Further, properties such as HMP degradation may be important to control the timing of cell release or their integration with the surrounding tissue environment. This may happen through the incorporation of hydrolytic or enzymatic cross-links or even through the use of phototriggered degradation processes<sup>118</sup>. In some cases, cells are made to adhere to the outside of HMPs or between populations of HMPs for delivery to tissues instead of encapsulated.

The cytocompatibility of the HMP encapsulation process is regulated by the method of gelation and the presence of shear forces, radicals and chemicals that may be harmful to cells. This is mostly similar to encapsulation of cells within bulk hydrogels, although there are some differences due to the fabrication processes to scale down the HMPs. For example, the use of lithography for HMP cell encapsulation does not impose significant added constraints compared to cell encapsulation within bulk hydrogels, and cell viability within such systems is generally high, at >90%<sup>58,59</sup>. However, achieving high cell viability within microfluidic emulsions is not trivial and depends on several factors, including the total batch-processing time, the pH of the precursor solution, the medium used to achieve effective droplet formation and the level of shear experienced by the precursor solution while travelling through the microfluidic channels.

Several approaches can be employed to improve cell viability when designing chips for microfluidic emulsions. First, the width of the channels should be carefully considered, as narrower channels (35  $\mu\text{m}$ ) resulted in significantly decreased cell viability compared to wider channels (100  $\mu\text{m}$ ), with viabilities of 71% and 91%, respectively<sup>33</sup>. The length of exposure to potentially harsh oil and surfactants can also decrease cell viability. The traditional approach to separate HMPs from oil is to apply cycles of centrifugation and washing steps; however, these processes can impact cell viability and reduce the yield of collected particles. Recently, a range of on-chip filtration processes to rapidly separate cross-linked HMPs from the continuous oil phase have been developed, and significant improvements in cell viability (up to 20%) have been reported<sup>119,120</sup>. Double-microfluidic-emulsion water-oil-water approaches have been used to generate cell-laden GelMA HMPs containing an ultra-thin oil shell on the particle that quickly dewets upon transfer into an aqueous solution<sup>121</sup>. This reduces cell exposure to the oil phase, resulting in improved viability compared to conventional, single-emulsion approaches. Oil-free, all-aqueous microfluidic approaches can also be used to generate HMPs based on the immiscibility between specific aqueous phases (such as PEG (30% w/v), sodium alginate (1% w/v) and dextran (15% w/v)<sup>122</sup>). An oil-free, centrifuge-based microfluidic device was also developed



that can produce alginate-based HMPs loaded with cells with viability as high as 70% (REFS<sup>48,123</sup>).

The distribution of cells within HMPs is another important consideration. Within emulsions, cell distributions may be influenced by HMP polydispersity (in batch emulsions) or long processing times (in microfluidics); however, increased control over the particle-production process and hydrogel cross-linking<sup>33,38,124</sup> and techniques that prevent cell settling in the hydrogel precursor solution can improve control over cell distributions<sup>125</sup>. Achieving consistent cell distributions with EHD-spraying techniques can also be challenging because excessive voltages may lead to cell aggregation towards the periphery of the HMPs<sup>79</sup>. Lithography approaches generally result in homogeneous cell distributions across particles, although particle cross-linking must occur sufficiently fast to prevent cell settling within the uncross-linked hydrogel precursor<sup>58</sup>.

**Applications of HMPs in cell delivery.**—HMPs have been used in a variety of cell applications, typically either as HMP suspensions or as granular hydrogels (often with low particle-packing density). The cell-laden HMPs may be cultured *in vitro* prior to delivery or delivered soon after cell encapsulation, and approaches often include co-cultures of cells. One major advantage of using HMPs for cell delivery is that cells are protected during the delivery process. Although bulk hydrogels may be injectable by exploiting shear thinning, shear forces acting on cells during injection may impact their viability<sup>126,127</sup>.

The shear-thinning behaviour of bulk hydrogels is based on the relative motion of adjacent polymer chains, which results in the transfer of shear forces to cells encapsulated within the hydrogel. In contrast, when cells are encapsulated in HMPs, the relative motion between particles during injection, especially in granular hydrogels, results in limited force transfer, which could enhance cell viability during extrusion through small needles. Although not specifically explored in a HMP system, hydrogel cross-linking has been shown to enhance cell protection during injection: lightly cross-linked alginate (~30 Pa) enhanced cell survival compared to non-cross-linked solutions<sup>128</sup>. In many HMPs, encapsulated cells are surrounded by a stable hydrogel, which likely improves cell viability during syringe delivery.

One area that has garnered attention is the use of HMPs to deliver bone-marrow-derived stromal cells (BMSCs) for the repair of bone defects. For example, injectable osteogenic microtissues were generated by encapsulating BMSCs and bone morphogenetic protein-2 (BMP-2) within GelMA HMPs fabricated using a microfluidic emulsion device<sup>129</sup>. Cells proliferated within the HMPs and, following delivery into a bone defect, induced robust bone regeneration<sup>129</sup>. In a similar approach, BMSCs were encapsulated in chitosan-collagen HMPs using a batch emulsion and differentiated along an osteogenic lineage *in vitro* before being delivered into mouse calvarial defects<sup>130</sup>. Predifferentiation of cells within the HMPs enhanced bone defect repair compared to undifferentiated controls, which demonstrates how HMP technologies can be used to deliver preformed, engineered microtissues that are otherwise challenging to deliver using minimally invasive techniques. A synergistic enhancement of bone formation was also observed when BMSCs and bone marrow

mononuclear cells were co-delivered by distinct chitosan-collagen HMP populations (fabricated by batch emulsion)<sup>131</sup>.

HMPs are also being explored as platforms for cell delivery in the repair of cartilage tissue. Early studies demonstrated that, following microencapsulation within HMPs, BMSCs differentiate along a chondrogenic lineage in the presence of the transforming growth factor  $\beta$ 3 (TGF- $\beta$ 3)<sup>132,133</sup>. Promising in vitro studies also reported enhanced synthesis of cartilage matrix components in gelatin-norbornene HMPs (produced by microfluidic emulsion) compared to cartilage synthesis promoted by bulk hydrogels, which was attributed to the microporosity among particles<sup>134</sup>. HMP systems have also been explored as templates for directing the repair of cartilage defects. For example, cartilage ECM-derived particles were fabricated by performing a series of fragmentation pulverization, sieving and decellularization steps on fresh cartilage tissues<sup>135</sup>. Following seeding with BMSCs, the ECM-derived particles promoted the repair of osteochondral defects in a rabbit model. In a similar study, chitosan-based and cellulose-based ECM mimetic nanofibrous microparticles were seeded with BMSCs to promote cartilage regeneration following delivery into chondral defects<sup>136</sup>.

HMPs have also been explored as platforms for delivering cells to promote cardiac repair. In one approach, cardiac side population cells (a progenitor cell in the heart) were seeded onto the surface of GelMA HMPs made using microfluidic emulsions<sup>35</sup>. The cells adhered and proliferated on the surface of the HMPs, and the inclusion of a silica hydrogel coating on the HMPs provided protection against oxidative stress to promote survival following delivery in vivo<sup>35</sup>. In another study, it was demonstrated that the delivery of cardiac progenitor cells (CPCs) to the ischaemic myocardium using gelatin HMPs enhanced cell engraftment compared to CPC-only controls<sup>137</sup>. Interestingly, despite improvements in cell engraftment, only marginal improvements in cardiac function were observed compared to the results obtained delivering CPC controls.

HMPs can also be used for applications in which physical isolation of transplanted cells from the immune system is required to promote a therapeutic effect following delivery in vivo. For example, delivery of insulin-producing islets has been widely explored for the treatment of diabetes; however, overcoming premature immune rejection following transplantation has been a major challenge. HMPs are an ideal platform for islet transplantation because they can be used to provide an immunoprotective barrier; the shorter diffusion distances (compared to those of bulk hydrogels) ensure the efficient exchange of nutrients and oxygen with the surrounding tissue to maintain islet survival and enhance the transfer of insulin from the islets to the surrounding vasculature<sup>138</sup>. Islets encapsulated in alginate HMPs (fabricated using EHD spraying) can be used as a platform to achieve immunoisolation and enhance the therapeutic window following delivery<sup>139</sup>. Interestingly, a size-dependent immune response was observed, with larger particles (up to 1.9 mm in diameter) promoting a reduced foreign-body response and fibrosis compared to smaller particles (500  $\mu$ m in diameter)<sup>139</sup>. An enhanced therapeutic window was achieved by co-delivering islets and PEG HMPs containing Fas ligand fabricated using microfluidic emulsions<sup>140</sup>. The Fas-ligand-containing HMPs localized immune suppression through

selective apoptosis of adaptive immune cells, which, in turn, promoted survival of the transplanted islets.

Although not developed specifically for delivery to tissues, the ability to structurally organize cells with predefined arrangements using microfluidic emulsions and lithography has made it possible to engineer in vitro models that mimic the complexity of in vivo microenvironments. Core-shell assemblies are promising for models in which homotypic and heterotypic interactions need to be balanced. For example, HMPs containing hepatocytes in the core and fibroblasts in the shell enhance the production of liver-specific functions compared to isolated or unstructured co-cultures<sup>46</sup>. In another experiment, pneumatic-aided imprint lithography was used to fabricate HMPs that mimicked the structural and cellular organization of a liver lobule with radially aligned hepatocytes and endothelial cells encapsulated in collagen<sup>124</sup>. It was demonstrated that the hepatocytes cultured within the structured 3D model were more sensitive to acetaminophen than those in unstructured 2D and 3D cultures, highlighting the influence of cell-cell and cell-ECM interactions in regulating in vitro drug-toxicity screening.

### HMPs for drug delivery

Hydrogels are very promising for the delivery of drugs (for example, small-molecule pharmaceuticals or growth factors), owing to their ability to protect, deliver and locally release bioactive factors in a controllable manner<sup>141</sup>, overcoming many of the limitations of traditional drug-administration methods (such as oral and intravenous) that often require high doses and repeated administration, and can lead to off-target effects. Traditionally, hydrogels for drug delivery have been macroscale bulk hydrogels, potentially delivered using minimally invasive techniques<sup>142,143</sup> and with controlled-release profiles<sup>3</sup>; however, the use of HMP systems is growing, owing, as discussed, to their distinct advantages over macroscale hydrogels. The small size of HMPs enables minimally invasive delivery through small needles and catheters<sup>8</sup> (FIG. 5), without the need for the specific in situ or shear-thinning cross-linking chemistries needed for the delivery of bulk hydrogels. Additionally, HMPs are highly versatile because multiple HMP populations can be easily combined to include multiple release profiles and degradation behaviours into a single injection<sup>9</sup>, which may be advantageous for many tissue-repair strategies to match biological signalling cascades. In this section, we discuss advances in the use of HMPs for drug delivery and highlight their increased versatility compared to traditional delivery strategies (FIG. 6).

**Controlling drug release from HMPs.**—The design of HMPs for drug delivery resembles that of bulk hydrogels, and the different strategies for controlling drug loading and release from bulk gels can be adapted to HMPs<sup>3</sup>. However, there are unique features that apply only to HMPs or affect them more than bulk systems. For example, microscale features such as the particle size and shape influence the total volume of cargo that can be encapsulated (FIG. 6a). The particle diameter is an important consideration; larger particles display more sustained release due to larger diffusion distances and smaller surface per hydrogel volume compared to smaller particles<sup>144,145</sup>. At the nanoscale, the particle mesh size influences drug diffusion through the network, and the release profile is slower for smaller mesh sizes<sup>146,147</sup>. Smaller mesh sizes can be achieved by increasing the polymer

concentration and cross-linking density during HMP formation. Finally, at the molecular scale, chemical interactions between the drug and hydrogel can be used to delay the release of cargo from the particle.

A range of interactions such as covalent conjugation and electrostatic and hydrophobic associations can be used to increase the drug-hydrogel affinity to control release<sup>3,148</sup>. For example, heparin, which is an important molecule in drug delivery because of its ability to reversibly bind proteins owing to its highly sulfated nature, has been incorporated into HMPs (using a batch-emulsion process) to sustain the delivery of BMP-2, vascular endothelial growth factor (VEGF) and basic fibroblast growth factor (FGF-2)<sup>149</sup>. Similar approaches can be adopted through sulfation of uronic acids that are present in commonly used hydrogels, such as hyaluronic acid and alginate<sup>150,151</sup>. For example, enhanced binding of growth factors within alginate HMPs has been achieved through sulfation<sup>152</sup>.

One advantage of using HMPs in drug delivery is that multiple particle populations can be mixed together to develop injectables with multifunctional behaviours. For example, two distinct drugs can be encapsulated in separate particle populations engineered with independent release profiles (FIG. 6b). Early work in this area demonstrated how the sequential release of distinct growth factors using HMP suspensions enhances tissue formation and repair<sup>153–155</sup>. Mixed particle populations containing different degradation behaviours can also be used to selectively deliver therapeutics in response to the local biological environment. For example, mixed hyaluronic-acid particle populations cross-linked with either stable or degradable cross-linkers (fabricated using a microfluidic emulsion) selectively degrade and release their cargo in response to the upregulated MMP activity present after myocardial infarction<sup>9</sup>. Further, spatial control over drug presentation following delivery is challenging to achieve using traditional injectable hydrogels. Recently, distinct populations of hyaluronic-acid HMPs formed using microfluidics were delivered in a spatially controlled manner by sequentially loading different particle populations into the syringe before injection<sup>104</sup>.

HMPs are often delivered as HMP composites, in which they are mixed into a secondary bulk hydrogel (FIG. 6b). Composite systems are appealing because they can address some of the limitations of both HMPs and macroscale hydrogels. For example, the secondary hydrogel can prevent particle migration from target sites when drug localization is required. As in heterogeneous particle systems, different drugs can be encapsulated into the HMPs and bulk hydrogels, with the drug release controlled by the independent properties of the two phases. Purely particle-based systems present short diffusion distances that can result in early ‘burst release’ of encapsulated drugs, whereas composite systems reduce burst effects by providing a secondary diffusional barrier around the particle phase<sup>156,157</sup>. HMP composites and bulk hydrogels are often exploited for their ability to trap cells in the hydrogel phase and drugs in the HMPs; HMPs loaded with growth factors have been used to direct the differentiation of stem cells encapsulated in the bulk hydrogel<sup>158,159</sup>. This makes it possible to create HMP composites containing distinct microscale and macroscale functionalities, with the growth-factor release controlled through HMP design, and the bulk hydrogel independently tunable to direct cell behaviour.

**Applications of HMPs in drug delivery.**—Due to their ease of injection and versatility, HMPs have been used in a wide variety of drug-delivery applications (FIG. 5). Many of the earliest applications were in the orthopaedic field, where HMP suspensions were used to provide sustained release of growth factors to promote bone and cartilage repair<sup>160,161</sup>. For example, genipin-cross-linked, gelatin-based microparticles, often made using batch emulsions, have been widely used to sustain the release of BMP-2 to promote bone repair<sup>162</sup>. Mixed particle populations have also shown promise for bone-repair applications. For example, the dual delivery of VEGF and BMP-2 using gelatin HMPs enhanced bone repair compared to the delivery of either factor alone<sup>163</sup>. In another example, oppositely charged chitosan particles formed using a batch emulsion were mixed to separately deliver osteoinductive and antibacterial factors in a sustained manner to promote bone regeneration<sup>164</sup>. The controlled delivery of chondroinductive factors, such as TGF- $\beta$ 1/3 and FGF-2 from gelatin particles, has been widely used for both cartilage-tissue engineering and cartilage-defect-repair applications<sup>165–167</sup>. HMP suspensions have also been explored for intraarticular delivery strategies: in a rat osteoarthritis model, degeneration of the articular surface was attenuated by delivering chitosan microparticles containing kartogenin (which can promote chondrogenesis) to the joint space<sup>168</sup>.

HMPs have also found utility in cardiac-repair applications, as they can be successfully delivered to the myocardium using minimally invasive, catheter-based strategies<sup>169</sup>. Following delivery, HMP suspensions provide sustained delivery of therapeutics to promote repair of the myocardium. For example, the sustained delivery of FGF from gelatin microspheres promoted angiogenesis and improved ventricular function in a model of myocardial infarction<sup>170,171</sup> and polyethylene glycol/polybutylene tere-phthalate (PEG-PBT) HMPs loaded with VEGF demonstrated a therapeutic effect when delivered after myocardial infarction<sup>172</sup>. More recently, it was demonstrated that hydrolytically degradable, hyaluronic-acid HMPs (engineered using a microfluidic emulsion) loaded with interleukin-10 promoted cardiac repair following delivery through a shear-thinning supramolecular hydrogel<sup>173</sup>.

HMPs are commonly used for pulmonary-drug-delivery applications because they can be fabricated with sizes suitable for bronchial-airway delivery ( $\sim 5 \mu\text{m}$ )<sup>174</sup>. Bulk hydrogels are not suitable for pulmonary delivery because of the risk of airway blockage. In an early experiment, alginate particles containing antitubercular drugs caused a nine-fold enhancement in drug bioavailability in the respiratory tract compared to bolus injection<sup>175</sup>. To facilitate sustained delivery to the lungs, therapeutics are often delivered via aerosols; aerodynamic particles with diameters of  $0.5\text{--}5 \mu\text{m}$  are required for deep lung penetration<sup>176</sup>. Upon penetration into the airways, the dried drug-loaded particles swell and increase in size once they are deposited on the moist surfaces of the lung<sup>177</sup>. Final sizes of  $>5 \mu\text{m}$  are required to avoid premature uptake and clearance by alveolar macrophages<sup>174</sup>. Reduced clearance rates can also be achieved by using particles that are mucoadhesive to provide sustained therapeutic delivery within the respiratory tract<sup>178</sup>. PEG HMPs (made by batch emulsion) have been developed that degrade in response to proteases (such as MMP-2) that are overexpressed in a range of pulmonary diseases, such as lung cancer, tuberculosis and chronic obstructive pulmonary diseases<sup>179,180</sup>.

For many years, effective and reliable oral insulin-delivery strategies have been sought for the treatment of diabetes. Hydrogels have been widely explored because they can protect insulin from degradation during the passage through the stomach, and release it in the intestinal system for transfer into the blood-stream<sup>181</sup>. HMP suspensions are ideal for insulin delivery because they can be administered orally and their small size enables easy passage to the intestine, where they offer a substantial surface-area coverage following delivery. A large body of work has focused on developing pH-responsive particles that can protect insulin from degradation while passing through the low-pH environment of the stomach, and then release their cargo to the small intestine, where the pH is higher<sup>181</sup>. One example is poly(methacrylic acid) (PMAA), which contains free carboxylic-acid groups that undergo pH-dependent protonation and deprotonation that leads to swelling and deswelling<sup>182–184</sup>. To delay particle clearance, mucoadhesive polymers such as chitosan can be incorporated into the HMPs<sup>185–187</sup>. Glucose-responsive particles that can release insulin in response to hyperglycaemic conditions have also been developed<sup>82</sup>: chitosan HMPs containing insulin and nanocapsules loaded with glucose-specific enzymes were prepared using EHD spraying. Their swelling changed under hyperglycaemic conditions as a result of the enzymatic conversion of glucose to gluconic acid, which led to protonation.

HMPs are also used as platforms for delivering growth factors within cell aggregates and microtissues. For example, gelatin HMPs loaded with TGF- $\beta$ 3 were embedded within mesenchymal stem/stromal cell (MSC) microtissues. HMPs were mixed with the cell suspension and then centrifuged; following aggregation, the particles were evenly distributed throughout the microtissues and supported levels of chondrogenic differentiation comparable to those obtained by exogenous delivery of the growth factor in the culture media<sup>147,188,189</sup>. Similar approaches have been used to control morphogen presentation (BMP4/noggin) within pluripotent stem-cell aggregates, including cases in which spatial control of the HMPs within the microtissue influenced the spatial differentiation of cells<sup>190</sup>.

### HMPs for building scaffolds

For nearly three decades, hydrogel scaffolds have been explored for numerous applications, including the repair and regeneration of tissues<sup>191,192</sup>. In many of these platforms for both in vitro and in vivo studies, cells are either embedded within the material during fabrication or seeded onto the scaffold after fabrication. Scaffolds must provide an environment that supports cell viability, enables desired cellular interactions (such as adhesion and remodelling), contains encapsulated soluble factors (such as growth factors, chemokines and cytokines) that control cellular outcomes and matches timescales relevant for tissue development and repair. Granular scaffolds are fabricated by packing HMPs until they reach a jammed state; as discussed, these systems are becoming popular because of their microporosity, injectability and tunability (FIG. 4). Granular scaffolds are inherently microporous, owing to the interstitial space among packed HMPs, which supports cellular invasion. By contrast, to allow for cell infiltration, bulk hydrogels must be engineered with features that permit material remodelling by the cells, which can lead to impaired mechanical properties over time. Granular scaffolds offer good potential for mechanical matching between tissue and scaffold, as well as long-lasting mechanical support for cells. This section explores the design of granular scaffolds and provides examples of their use.



**Designing granular scaffolds.**—As with drug-delivery systems, the design of granular scaffolds borrows many concepts originally developed for bulk-hydrogel systems<sup>3,193</sup>. Of particular interest for granular scaffolds are HMP annealing methods, the resulting HMP and bulk mechanical properties and the incorporation of adhesion and other bioactive signals (FIG. 7). Many granular scaffolds are made of HMPs annealed to each other to provide stabilization in the presence of excessively aqueous environments or mechanical agitation. Annealing granular scaffolds results in MAP scaffolds<sup>8</sup>. In wet, cutaneous wounds, annealing is often essential to limit inflammation and promote wound closure<sup>8</sup>. The annealing chemistry offers further control over the engineering of HMPs, and various covalent, reversible and electrostatic bonds have been explored (FIG. 7a). There are numerous cross-links per HMP, and, thus, increased cross-linking results in a more stable and rigid scaffold. Covalent bonds result in the most stable scaffolds, with more robust mechanical properties (such as storage and Young's modulus) compared to scaffolds comprising non-annealed HMPs or HMPs annealed with non-covalent bonds. Covalent cross-linking has been achieved by a variety of chemistries, including enzymatic (FXIIIa) chemistry<sup>8,10,54</sup>, carboxylic/amine chemistry<sup>10,134</sup>, light-mediated radical reactions<sup>10,194</sup>, light-mediated thiol-ene reactions<sup>195</sup>, azide/alkyne click chemistry<sup>106</sup> and norbornene-tetrazine cycloadditions<sup>15,98</sup>. An example of reversible bonds are host-guest interactions based on cyclodextrin-adamantine; for example, hyaluronic-acid HMPs (made using a microfluidic emulsion) were modified with adamantane and then bonded together with cyclodextrin-modified polymers<sup>9</sup>. The reversibility of these host-guest bonds causes the material to flow upon shear stress, allowing for its injectability, followed by self-healing, during which gel properties are recovered after the shear is removed. Similar shear-thinning and self-healing behaviours are observed when HMPs are annealed using electrostatic interactions between HMPs, which are particularly appealing due to their simplicity<sup>196</sup>.

Mechanical properties are important bioactive cues for cells both in vitro and in vivo; thus, their modulation is of particular interest. The mechanical properties of MAP scaffolds can be modified by modulating the stiffness of individual HMPs, the chemistry of annealing, the amount of annealing between HMPs and the particle-packing density (FIG. 7b). The method of annealing can modify the bulk mechanics without influencing the local mechanics; thus, MAP scaffolds can present different mechanical cues at the local and bulk levels. Individual HMP stiffness can be tuned during fabrication by increasing the material concentration or degree of polymer cross-linking<sup>98,195</sup>; MAP scaffolds produced from HMPs with different stiffnesses influence cell behaviour differently: stiffer particles generally lead to increased cell spreading and proliferation<sup>54,98</sup>. The incorporation of soft-to-stiff gradients in PEG HMPs (produced by microfluidic emulsion) led to fibroblast migration towards the stiff end of the material<sup>54</sup>. By layering HMP species of varying stiffnesses in a syringe or catheter, material gradients may be produced upon injection, owing to the unique jamming properties of granular hydrogels (FIG. 7c). System-wide stiffness is further affected by the particle-packing density. Increasing particle-packing density generally leads to increased stiffness, but if HMPs are packed 'beyond jamming' so that they deform and lose interstitial space, they no longer function as a scaffold and, instead, exhibit characteristics similar to those of bulk hydrogels<sup>92</sup>. The HMP-packing density can be modulated by changing the particle-

settling time before annealing<sup>10</sup> or by removing liquid from the particle suspension via vacuum or centrifugation.

The local geometry of a cell's microenvironment also plays a role in modulating cell behaviour<sup>197–199</sup>. In granular scaffolds, HMP surfaces and the void space among particles comprise the microarchitecture of the cellular environment. Therefore, the size and shape of HMPs, which instructs the porosity of the system, may influence cell behaviour (FIG. 7d). Seeding fibroblast cells on different MAP scaffolds comprising spherical HMPs (hyaluronic acid-PEG produced using a batch emulsion followed by sieving) that ranged in diameter from small (20–60  $\mu\text{m}$ ), medium (60–100  $\mu\text{m}$ ) and large (100–200  $\mu\text{m}$ ) highlighted differences in cell spreading and proliferation depending on HMP size. In the large-particle group, cells visibly wrapped around large particles and adopted a more flattened shape<sup>98</sup>. These results were attributed to the differences in pore sizes and HMP surface area available to cells. Similarly, seeding stromal cells in MAP scaffolds comprising HMPs with diameters of 10  $\mu\text{m}$  or 100  $\mu\text{m}$  led to increased spreading of cells in the scaffolds with larger HMPs<sup>106</sup>.

The engineering of integrin-binding cues within materials remains essential for many cellular responses in vitro and in vivo, such as angiogenesis<sup>200</sup>. Functionalizing HMP polymers with integrin-binding peptides, such as arginine-glycine-aspartic acid (RGD), has proven crucial to improve cell affinity for HMP surfaces. As in bulk hydrogel scaffolds, the concentration and spatial distribution of integrin-binding proteins within HMPs affects cellular responses (FIG. 7e). For example, increasing the concentration of RGD per HMP resulted in increased cell spreading and proliferation<sup>98</sup>.

As in 2D cultures<sup>201</sup>, the presentation of RGD is important; RGD islands spaced too far apart or excessively homogeneously distributed resulted in ineffective binding<sup>98</sup>. In addition to adhesion, the degradation of HMPs is also an important material feature to control, for example through the inclusion of cross-links that respond to local enzymes<sup>9</sup>. The mixing of particles with variable modes of degradation results in selective HMP degradation from a scaffold, which again highlights the importance of heterogeneity in the use of HMPs in biomedical applications.

**Applications of granular scaffolds.**—The use of granular HMP scaffolds in tissue repair has grown extensively in recent years. Most of the earliest works utilizing granular scaffolds were focused on bone and cartilage tissue engineering<sup>202–204</sup>. In one study, large chitosan hydrogel particles with diameters in the millimetre range were annealed to form a granular scaffold for osteoblast seeding<sup>204</sup>. Since this work, the applications of granular scaffolds have expanded; here, we present a number of applications in the context of in vivo wound healing, as well as ex vivo cell studies.

Granular scaffolds are promising for the promotion of wound healing in numerous tissues (FIG. 7f). The first use of MAP scaffolds was in a seminal study comparing them to a bulk hydrogel in a murine, cutaneous-wound-healing model<sup>8</sup>. PEG-based HMPs made using a microfluidic emulsion were injected into cutaneous-tissue defects and then covalently annealed in vivo using factor XIII-mediated K and Q peptide amide linkages. The presence of the MAP scaffold not only accelerated re-epithelialization but, five days post injection,

the wound bed displayed hair follicles and sebaceous glands — structures that are characteristically not seen in scar tissue — which indicated a truly regenerative process. Such results could not be obtained with non-annealed HMP gels. These surprising findings led to several subsequent applications of MAP scaffolds. Hyaluronic-acid-based HMPs were designed to covalently anneal in vivo after being applied to stroke cavities induced in mice<sup>103</sup>. Within ten days from injection, the MAP scaffolds showed vascularization and neural progenitor cell migration towards the wound site, suggesting a tissue remodelling response. MAP scaffolds have also been engineered into modular implants to accommodate the long, narrow geometry of axon defects found in spinal-cord injuries<sup>205</sup>. PEG-based HMPs made using a batch emulsion were moulded around narrow cylinders and covalently annealed, after which the cylinder was removed to create a tubular scaffold containing a hollow lumen that provided directional guidance for growing axons. Stacked tubes implanted into spinal-cord defects in mice showed a reduction of glial scarring compared to a bulk hydrogel control, suggesting regenerative potential due to the scaffold microstructure.

Non-covalent, reversible annealing techniques have also been used for MAP materials in vivo. A self-healing cross-linking method involving host-guest interactions was developed to assemble hyaluronic-acid-based HMPs<sup>9</sup>. Heterogeneity was explored by experimenting with HMP species that differed in degradability and payload. Delivery to infarcted cardiac tissue in rats demonstrated a two-component response that resulted in successful interaction with inflammatory cells. Granular scaffolds have also been used in bone repair in more recent studies, in which packed heparin-modified gelatin HMPs produced using a batch emulsion were applied to rat mandibular-bone defects in a type 2 diabetes mellitus model<sup>206</sup>. The HMPs were loaded with IL-4 to polarize macrophages towards an anti-inflammatory phenotype, which successfully reduced the inflammation, enhancing osteogenesis and promoting a regenerative state. There is consensus among these studies that the microporosity of granular scaffolds plays a significant role in the improved cellular responses.

The microporosity of granular hydrogels, the ability of cells to spread without scaffold degradation and the tunability of HMPs makes granular scaffolds ideally suited as 3D culturing devices for studying cell behaviour in vitro. Cells can be seeded on top of granular hydrogels to capture information about cell infiltration or they can be mixed with the HMPs to observe their responses, such as spreading, proliferation and multicellular structure formation (FIG. 7g). Mesenchymal stem cells were loaded inside the HMPs of a MAP scaffold to study maturation and long-term maintenance of the cells within the scaffold. The results showed an upregulation of chondrogenic gene expression and the presence of hyaline-like cartilage tissue surrounding the gelatin-norbornene HMPs (made by microfluidic emulsion)<sup>134</sup>. MAP scaffolds formed using hyaluronic acid-PEG HMPs (made by batch emulsion) have also been studied as a framework for gene transfer because tunable changes in the MAP microenvironment influence cell behaviour, which, in turn, impacts transfection dynamics<sup>15</sup>.

The modular properties of granular systems have been leveraged to engineer scaffolds containing property gradients for improved tissue repair. For example, three forms of PEG HMPs with different functionalities were used to form scaffolds: the first provided

mechanical support, the second provided controlled delivery of the angiogenesis-promoting molecule (sphingosine 1-phosphate) and the third acted as a porogen to impose pockets of macroporosity in the scaffold<sup>16</sup>. Gradients in scaffold porosity were produced by increasing the porogen fraction through the depth of the scaffold, which promoted endothelial cell migration into the construct. Using a similar approach, gradients of glial-cell-derived human neurotrophic factor were produced using heparinated PEG HMPs for nerve-regeneration applications<sup>207</sup>. Different cross-linking densities were used to tune the rate of growth-factor release within each region of the scaffold, which led to the formation of a growth-factor gradient. The graded scaffolds promoted axonal regeneration following implantation into severed sciatic nerves<sup>207,208</sup>.

Lastly, as a prelude to microtissue-like cell-transplant platforms, MAP scaffolds that utilize cells themselves to anneal HMPs have been developed<sup>209,210</sup>. In these applications, HMP surfaces are modified to accommodate cell adhesion. One approach also adopted a method called thermoswitching to influence the cell-release dynamics<sup>210</sup>.

### HMPs for biofabrication

HMPs have also been used in biofabrication, where additive manufacturing is used to develop in vitro models or implantable constructs that mimic the complexity of native tissues<sup>211</sup>. Biofabrication processes can be categorized as either bioassembly, in which preformed building blocks are assembled into 3D constructs using an automated-assembly technology, or bioprinting, in which extrusion-based and lithography-based printing techniques are used to build 3D structures<sup>212</sup>. Some of the earliest examples of HMPs in biofabrication involved bioassembly, in which cell-encapsulating HMPs were used as building blocks in automated-assembly approaches (FIG. 8). In an early example, a fluidic-based bioassembly process was developed in which railed microfluidic channels were used to guide the movement of PEGDA HMPs into 3D constructs<sup>57</sup> (FIG. 8a). External magnetic fields have also been leveraged to guide magnetic-nanoparticle-loaded GelMA and PEG HMPs into multilayered 3D structures<sup>213</sup>, and untethered, magnetically responsive microrobots were used to manipulate HMPs into 3D assemblies<sup>214</sup> (FIG. 8b). Acoustic-wave technologies can also be used to manipulate HMPs to assemble 3D constructs<sup>215</sup> (FIG. 8c).

HMPs have also been used in the production of bioinks for extrusion-based bioprinting. Traditionally, extrudable bioinks are prepared using single-network or double-network hydrogels, and their biophysical and biochemical properties are kept homogeneous; however, heterogeneity may be desirable for printing complex tissues. To address this limitation, PEG HMPs (made using microfluidics) were combined with an extrudable bulk hydrogel precursor to engineer a composite bioink platform containing distinct microscale and macroscale environments<sup>216</sup>. The modular nature of the system was demonstrated by encapsulating MSCs in the PEG HMPs, which were then surrounded by a proangiogenic bulk hydrogel composed of fibrin loaded with endothelial cells. Further advances in this area should enable the development of a diverse set of multifunctional bioinks in which the local microenvironment can be tailored for distinct encapsulated cell types and/or bioactive factors.

More recently, it has been demonstrated that extrudable bioinks can be made from granular hydrogels<sup>7,217</sup>. When HMPs are packed closely together in a jammed state, they behave as a solid, but when external forces are applied, they display fluidic collective movement. This shear-thinning behaviour has been exploited for extrusion bioprinting because it enables extrusion through a needle and immediate post-printing stabilization<sup>7,217</sup> (FIG. 8d,e). Inks for extrusion bioprinting have generally been engineered at the molecular scale, often leveraging reversible cross-linking chemistries. However, the shear-thinning behaviour of jammed HMPs is based predominately on the physical interactions between particles, which expands the range of materials that can be extruded<sup>7,217</sup>. Another advantage of HMP-based inks is their inherently modularity: multiple particle populations can be fabricated and then jammed together. Further, the HMPs themselves can be cross-linked to stabilize the final printed structure.

Traditional extrusion-bioprinting approaches involve layer-by-layer printing onto a 2D surface. However, because the printed structure is under the influence of gravity, it is challenging to print complex structures with high aspect ratios in the vertical direction. Gel-in-gel printing approaches have been developed in which inks are directly extruded into a secondary support hydrogel that serves to minimize the effect of gravity<sup>218</sup> (FIG. 8f). This enables the printing of taller, more complex 3D structures. Jammed HMP systems are an ideal support for gel-in-gel printing because, during extrusion, the particles around the translating nozzle locally displace to support the ink and printed object<sup>219</sup>. The most commonly used support hydrogel for 3D printing is Carbopol, which is a commercial, particle-based hydrogel composed of poly(acrylic acid) HMPs (average diameter 0.2  $\mu\text{m}$ ). Carbopol-support hydrogels are compatible with a wide range of bioinks and can be used to print diverse, multicellular structures<sup>220</sup>. Support hydrogels for 3D printing have also been made using a granular gelatin HMP system prepared by fragmentation<sup>86</sup>.

### Other applications of HMPs

HMP suspensions and granular hydrogels have been utilized in applications that extend beyond those previously discussed. For decades, hydrogels (in particular, hyaluronic acid) have been used in the cosmetic industry as dermal fillers for soft-tissue augmentation owing to their injectability, swelling and consistency that is similar to that of human cutaneous tissue<sup>221,222</sup>. Hydrogel fillers are commonly manufactured by forcing a bulk gel through a fine screen (mechanical fragmentation). The resulting HMPs are then either mixed with additional polymer solution to reduce interparticle friction for smoother injection or left as packed particles. Smaller particles make for better superficial fillers that target wrinkles or scar divots, whereas larger particles are used for deep-tissue volumizers<sup>221</sup>. Products on the market vary in terms of formulation, manufacturing techniques, consistency, degradation times, intended usage and cost.

Owing to their micrometre size scale and tunable units, HMPs have also proved useful as microtopo-graphical cues for cells. HMPs delivered to damaged tissue serve as local anchor points for cell adhesion and contact guidance that help to restore the mechanical properties of the ECM. Microrod suspensions (100  $\mu\text{m}$ ) made from hyaluronic acid were fabricated for this purpose using a lithographical process and were delivered to fibrotic cardiac tissue in

rats<sup>105</sup>. Previous work showed that a minimal elastic modulus of 20 kPa was necessary for microrod HMPs to elicit fibroblast cell responses, indicating the importance of material stiffness for topographical applications. The hyaluronic-acid HMPs stimulated attachment by local cells, discouraged the pro-scarring myofibroblast phenotype and resulted in improved organ function<sup>105</sup>. In an attempt to target the linear, directional aspect of nerve cells, an HMP composite material was developed containing PEG acrylate microrod HMPs (made by lithography) that were laced with small amounts of superparamagnetic nanoparticles, which allowed for HMP alignment in an external magnetic field<sup>223</sup>. The microrod HMPs could align fibroblasts and unidirectionally guide nerve cells in vitro, demonstrating the efficacy of targeting contact guidance to influence cell behaviour. Much work has also been done to study how HMPs can be used as microstructures that offer environmental heterogeneity in terms of stiffness and topography both in vitro and in vivo<sup>224</sup>.

Inspired by synthetic-cell biology, HMPs have recently been engineered to contain multiple compartments that mimic distinct organelles within a cell. For example, microfluidics was used to fabricate PEG-based HMPs containing two compartments<sup>225</sup>. Each compartment was designated for a single chemical reaction and the product from the first compartment was used as reactant for the second. Reactions in each compartment were pH-specific to demonstrate effective compartmentalization. The elegantly designed synthetic cells were highly successful at performing their task and showcased the potential for new, 'smart' HMP technologies.

## Future perspectives

We have covered the main classes of HMP systems, the fabrication techniques to manufacture them, their properties across length scales and a number of their biomedical applications. Overall, their injectability, modular design and porosity constitute clear advantages over traditional bulk hydrogels in many applications. Advances are expected across all areas discussed, particularly as new fabrication methods make diverse HMPs accessible to a broad user base and as new reports generate further enthusiasm for their use.

Regarding HMPs fabrication, microfluidic technologies and other techniques will continue to improve, allowing for the scaling up of HMP fabrication with uniform particle populations and batch-to-batch consistency at high production rates. Recent years have already seen a scaling up of microfluidic platforms with these goals in mind<sup>33,226</sup>, and additional advances will likely allow the fabrication of heterogeneous HMP systems on a single chip by controlling hydrogel precursor flows and mixing. With these advances plus improved material consistency, the characterization of HMP-based biomaterials (based on numerous microscopy and rheological methods) will also improve, including better visualization of individual HMPs and their interactions under mechanical load. Broadening the classes of materials used to make HMPs will expand the material properties of HMP systems, for example introducing stimuli-responsive materials that change under various endogenous and exogenous signals.



To better design and understand HMP systems, computational models and numerical approaches will be useful. For example, multiscale models have been developed that use the discrete element method to capture behaviour that follows Newtonian mechanics at the microscopic level (for granular and composite systems) and then either the finite difference method or elasto-plasticity theory to model behaviour that follows continuum mechanics at the macroscopic level<sup>227,228</sup>, where, ultimately, first-order homogenization and kinematic averaging are used to couple the two. Such computational approaches offer a deeper understanding for how granular systems respond to mechanical loading, and many more approaches have and can be used to aid in predicting bulk material properties and behaviours, as well as local internal, featural structures. Computational models and numerical simulations will be invaluable in both expediting experimental design and analysing fabricated materials.

Beyond the fabrication and understanding of HMP systems, the applications of these materials will likely broaden as more investigators recognize their advantages. Already, HMP systems have been inhaled, ingested, injected into intraarticular space and injected into tissues (such as dermal, neural and muscle tissues). Additionally, with rapid advances in stem-cell and drug-design technologies (such as the discovery of induced pluripotent stem cells and CRISPR), the options for HMP cargo will continue to grow. A major concern with the use of the CRISPR technology is off-target effects, so approaches that enable precise activation within targeted tissues are desirable<sup>229</sup>. It is possible that the versatility and modularity of HMP systems will provide a platform for controlling and localizing the activity of CRISPR-Cas9 following delivery in vivo. As discussed, the potential complexity of mixing many particle populations has only been briefly investigated, despite their immense potential for delivering sequential signals to tissues and cells.

HMP systems are also likely to be developed with new and interesting properties. The properties of native tissues (such as bone and cartilage) are often the result of interactions between multiple tissue components across multiple length scales. Granular systems offer a modular platform for recreating physical and chemical properties that can be independently controlled across these length scales, which include the nanoscale (hydrogel mesh size), microscale (interparticle interactions) and macroscale (particle-packing fraction). It has already been demonstrated that interparticle motion can induce shear-thinning behaviour, and that static<sup>8</sup> and dynamic<sup>85</sup> interparticle cross-links can be used to alter particle rearrangements under load. Further advances in this area will likely lead to the creation of a novel class of materials that better mimic the multiscale mechanical behaviour of native tissues.

Recent technological advances have enabled the analysis of complex biological systems at the single-cell level. Microfluidic technologies are being used for cell separation during single-cell sequencing, and it was demonstrated that single cells can be encapsulated in thin and tunable HMPs using microfluidics<sup>112</sup>. This area is likely to continue advancing, and this technology opens up numerous avenues for biological exploration. For example, the screening of biological cues (stiffness, viscoelasticity or drug concentration) is typically only explored across a small range of parameters and is usually based on conventional bulk assays that mask cell-to-cell variability. The integration of HMPs and sequencing

technologies could enable high-throughput screening at the single-cell level to understand responses to multiple biophysical environments or drugs, as well as the interplay between cells in these environments.

We have only scratched the surface in terms of discussing the use of HMPs for scaffold building in vitro and in vivo. Besides performing more experiments to understand how the fine-tuning of physical and biochemical properties (such as mixing different HMP formulations) affects cells within MAP scaffolds, there are opportunities to explore features of MAP scaffolds that are not present in bulk hydrogels. For example, the local-void-space geometry within MAP systems has been minimally studied and almost exclusively in the context of spherical HMPs of different sizes. It would be interesting to more rigorously analyse local geometry formed from non-spherical or non-convex HMP shapes to gain more general knowledge about the role of void-space geometry on cell behaviour, multicellular arrangements and endogenous repair. Compared to bulk systems, the versatility of HMP systems makes them appealing as platforms to target endogenous repair processes that are spatially and temporally complex. The ability to form multiple microenvironments within a MAP scaffold by combining fractions of HMPs with different properties (such as stiffness or loading with bioactive cues) can give rise to superior organoid culture systems and endogenous repair through the generation of spatiotemporal microgradients.

Lastly, the use of HMPs for biofabrication is still in its infancy, with jammed HMP systems leveraged for extrusion bioprinting<sup>7</sup> and individual HMPs having been patterned using a range of bioassembly technologies<sup>213,215</sup>. The shear-thinning behaviour of jammed HMPs is based on the physical interactions between the particles; thus, the range of materials that can be processed with extrusion printing will likely expand. In addition, the modularity of jammed systems will probably enable the preparation of more diverse inks with multifunctional behaviours. Acoustic, robotic and magnetic guidance of HMPs have only been explored in relatively 2D systems within the bioassembly field; further advances in this area will enable high-resolution positioning within 3D systems. Overall, there are likely important developments ahead in the field of HMPs for biomedical applications.

## Acknowledgements

J.A.B. acknowledges funding through the National Science Foundation through the PENN MRSEC (DMR-1720530) and STC Program (CMMI: 15-48571). T.S. acknowledges funding from the National Institutes of Health (R01NS094599) and Duke Biomedical Engineering. The authors would like to thank their laboratories for the helpful input and suggestions on the manuscript.

## References

1. Caliani SR & Burdick JA A practical guide to hydrogels for cell culture. *Nat. Methods* 13, 405–414 (2016). [PubMed: 27123816]
2. Van Vlierberghe S, Dubruel P & Schacht E Biopolymer-based hydrogels as scaffolds for tissue engineering applications: a review. *Biomacromolecules* 12, 1387–1408 (2011). [PubMed: 21388145]
3. Li J & Mooney DJ Designing hydrogels for controlled drug delivery. *Nat. Rev. Mater* 1, 16071 (2016). [PubMed: 29657852]
4. Annabi N et al. Controlling the porosity and microarchitecture of hydrogels for tissue engineering. *Tissue Eng. Part B Rev* 16, 371–383 (2010). [PubMed: 20121414]

5. Henderson TMA, Ladewig K, Haylock DN, McLean KM & O'Connor AJ Cryogels for biomedical applications. *J. Mater. Chem. B* 1, 2682–2695 (2013). [PubMed: 32260973]
6. Wade RJ, Bassin EJ, Rodell CB & Burdick JA Protease-degradable electrospun fibrous hydrogels. *Nat. Commun* 6, 6639 (2015). [PubMed: 25799370]
7. Highley CB, Song KH, Daly AC & Burdick JA Jammed microgel inks for 3D printing applications. *Adv. Sci* 6, 1801076 (2019).
8. Griffin DR, Weaver WM, Scumpia PO, Di Carlo D & Segura T Accelerated wound healing by injectable microporous gel scaffolds assembled from annealed building blocks. *Nat. Mater* 14, 737–744 (2015). [PubMed: 26030305]
9. Mealy JE et al. Injectable granular hydrogels with multifunctional properties for biomedical applications. *Adv. Mater* 30, 1705912 (2018).
10. Sideris E et al. Particle hydrogels based on hyaluronic acid building blocks. *ACS Biomater. Sci. Eng* 2, 2034–2041 (2016). [PubMed: 33440539]
11. Franco CL, Price J & West JL Development and optimization of a dual-photoinitiator, emulsion-based technique for rapid generation of cell-laden hydrogel microspheres. *Acta Biomater* 7, 3267–3276 (2011). [PubMed: 21704198]
12. Leong W, Lau TT & Wang DA A temperature-cured dissolvable gelatin microsphere-based cell carrier for chondrocyte delivery in a hydrogel scaffolding system. *Acta Biomater* 9, 6459–6467 (2013). [PubMed: 23142479]
13. Liu AL & Garcia AJ Methods for generating hydrogel particles for protein delivery. *Ann. Biomed. Eng* 44, 1946–1958 (2016). [PubMed: 27160672]
14. Xu Q et al. Preparation of monodisperse biodegradable polymer microparticles using a microfluidic flow-focusing device for controlled drug delivery. *Small* 5, 1575–1581 (2009). [PubMed: 19296563]
15. Truong NF, Leshner-Pérez SC, Kurt E & Segura T Pathways governing polyethylenimine polyplex transfection in microporous annealed particle scaffolds. *Bioconj. Chem* 30, 476–486 (2019). [PubMed: 30513197]
16. Scott EA, Nichols MD, Kuntz-Willits R & Elbert DL Modular scaffolds assembled around living cells using poly(ethylene glycol) microspheres with macroporation via a non-cytotoxic porogen. *Acta Biomater* 6, 29–38 (2010). [PubMed: 19607945]
17. Stenekes RJH, Franssen O, van Bommel EMG, Crommelin DJA & Hennink WE The preparation of dextran microspheres in an all-aqueous system: effect of the formulation parameters on particle characteristics. *Pharm. Res* 15, 557–561 (1998). [PubMed: 9587951]
18. Elbert DL Liquid–liquid two-phase systems for the production of porous hydrogels and hydrogel microspheres for biomedical applications: a tutorial review. *Acta Biomater* 7, 31–56 (2011). [PubMed: 20659596]
19. Nichols MD, Scott EA & Elbert DL Factors affecting size and swelling of poly(ethylene glycol) microspheres formed in aqueous sodium sulfate solutions without surfactants. *Biomaterials* 30, 5283–5291 (2009). [PubMed: 19615738]
20. Jeon O, Wolfson DW & Alsberg E In-situ formation of growth-factor-loaded coacervate microparticle-embedded hydrogels for directing encapsulated stem cell fate. *Adv. Mater* 27, 2216–2223 (2015). [PubMed: 25708428]
21. Thorsen T, Roberts RW, Arnold FH & Quake SR Dynamic pattern formation in a vesicle-generating microfluidic device. *Phys. Rev. Lett* 86, 4163–4166 (2001). [PubMed: 11328121]
22. Anna SL, Bontoux N & Stone HA Formation of dispersions using “flow focusing” in microchannels. *Appl. Phys. Lett* 82, 364–366 (2003).
23. De Geest BG, Urbanski JP, Thorsen T, Demeester J & De Smedt SC Synthesis of monodisperse biodegradable microgels in microfluidic devices. *Langmuir* 21, 10275–10279 (2005). [PubMed: 16262275]
24. Pittermannová A et al. Microfluidic fabrication of composite hydrogel microparticles in the size range of blood cells. *RSC Adv* 6, 103532–103540 (2016).
25. Utada AS et al. Monodisperse double emulsions generated from a microcapillary device. *Science* 308, 537–541 (2005). [PubMed: 15845850]

26. Nisisako T & Torii T Microfluidic large-scale integration on a chip for mass production of monodisperse droplets and particles. *Lab Chip* 8, 287–293 (2008). [PubMed: 18231668]
27. Kim J-W, Utada AS, Fernández-Nieves A, Hu Z & Weitz DA Fabrication of monodisperse gel shells and functional microgels in microfluidic devices. *Angew. Chem* 119, 1851–1854 (2007).
28. Greenwood-Goodwin M, Teasley ES & Heilshorn SC Dual-stage growth factor release within 3D protein-engineered hydrogel niches promotes adipogenesis. *Biomater. Sci* 2, 1627–1639 (2014). [PubMed: 25309741]
29. Foster GA et al. Protease-degradable microgels for protein delivery for vascularization. *Biomaterials* 113, 170–175 (2017). [PubMed: 27816000]
30. Deveza L et al. Microfluidic synthesis of biodegradable polyethylene-glycol microspheres for controlled delivery of proteins and DNA nanoparticles. *ACS Biomater. Sci. Eng* 1, 157–165 (2015). [PubMed: 33429514]
31. Jiang W, Li M, Chen Z & Leong KW Cell-laden microfluidic microgels for tissue regeneration. *Lab Chip* 16, 4482–4506 (2016). [PubMed: 27797383]
32. Selimovi Š, Oh J, Bae H, Dokmeci M & Khademhosseini A Microscale strategies for generating cell-encapsulating hydrogels. *Polymers* 4, 1554–1579 (2012). [PubMed: 23626908]
33. Headen DM, García JR & García AJ Parallel droplet microfluidics for high throughput cell encapsulation and synthetic microgel generation. *Microsyst. Nanoeng* 4, 17076 (2018).
34. Koster S et al. Drop-based microfluidic devices for encapsulation of single cells. *Lab Chip* 8, 1110–1115 (2008). [PubMed: 18584086]
35. Cha C et al. Microfluidics-assisted fabrication of gelatin-silica core-shell microgels for injectable tissue constructs. *Biomacromolecules* 15, 283–290 (2014). [PubMed: 24344625]
36. Jiang Z, Xia B, McBride R & Oakey J A microfluidic-based cell encapsulation platform to achieve high long-term cell viability in photopolymerized PEGNB hydrogel microspheres. *J. Mater. Chem. B* 5, 173–180 (2017).
37. Kumachev A, Tumarkin E, Walker GC & Kumacheva E Characterization of the mechanical properties of microgels acting as cellular microenvironments. *Soft Matter* 9, 2959–2965 (2013).
38. Headen DM, Aubry G, Lu H & Garcia AJ Microfluidic-based generation of size-controlled, biofunctionalized synthetic polymer microgels for cell encapsulation. *Adv. Mater* 26, 3003–3008 (2014). [PubMed: 24615922]
39. Allazetta S, Hausherr TC & Lutolf MP Microfluidic synthesis of cell-type-specific artificial extracellular matrix hydrogels. *Biomacromolecules* 14, 1122–1131 (2013). [PubMed: 23439131]
40. Seiffert S, Thiele J, Abate AR & Weitz DA Smart microgel capsules from macromolecular precursors. *J. Am. Chem. Soc* 132, 6606–6609 (2010). [PubMed: 20397695]
41. Seiffert S & Weitz DA Microfluidic fabrication of smart microgels from macromolecular precursors. *Polymer* 51, 5883–5889 (2010).
42. Chu LY, Utada AS, Shah RK, Kim JW & Weitz DA Controllable monodisperse multiple emulsions. *Angew. Chem. Int. Ed* 46, 8970–8974 (2007).
43. Seiffert S, Romanowsky MB & Weitz DA Janus microgels produced from functional precursor polymers. *Langmuir* 26, 14842–14847 (2010). [PubMed: 20731338]
44. Zhao CX Multiphase flow microfluidics for the production of single or multiple emulsions for drug delivery. *Adv. Drug Deliv. Rev* 65, 1420–1446 (2013). [PubMed: 23770061]
45. Duncanson WJ et al. Microfluidic synthesis of advanced microparticles for encapsulation and controlled release. *Lab Chip* 12, 2135–2145 (2012). [PubMed: 22510961]
46. Chen Q et al. Controlled assembly of heterotypic cells in a core-shell scaffold: organ in a droplet. *Lab Chip* 16, 1346–1349 (2016). [PubMed: 26999495]
47. Zhang L et al. Microfluidic templated multicompartment microgels for 3D encapsulation and pairing of single cells. *Small* 14, 1702955 (2018).
48. Yoshida S, Takinoue M & Onoe H Compartmentalized spherical collagen microparticles for anisotropic cell culture microenvironments. *Adv. Healthc. Mater* 6, 1601463 (2017).
49. Kamperman T, Trikalitis VD, Karperien M, Visser CW & Leijten J Ultrahigh-throughput production of monodisperse and multifunctional Janus microparticles using in-air microfluidics. *ACS Appl. Mater. Interfaces* 10, 23433–23438 (2018). [PubMed: 29952552]

50. Visser CW, Kamperman T, Karbaat LP, Lohse D & Karperien M In-air microfluidics enables rapid fabrication of emulsions, suspensions, and 3D modular (bio)materials. *Science Adv* 4, eaao1175 (2018).
51. Bardin D, Kendall MR, Dayton PA & Lee AP Parallel generation of uniform fine droplets at hundreds of kilohertz in a flow-focusing module. *Biomicrofluidics* 7, 034112 (2013).
52. Muluneh M & Issadore D Hybrid soft-lithography/laser machined microchips for the parallel generation of droplets. *Lab Chip* 13, 4750–4754 (2013). [PubMed: 24166156]
53. Li W, Greener J, Voicu D & Kumacheva E Multiple modular microfluidic (M3) reactors for the synthesis of polymer particles. *Lab Chip* 9, 2715–2721 (2009). [PubMed: 19704988]
54. de Rutte JM, Koh J & Di Carlo D Scalable high-throughput production of modular microgels for in situ assembly of microporous tissue scaffolds. *Adv. Funct. Mater* 29, 1900071.
55. Helgeson ME, Chapin SC & Doyle PS Hydrogel microparticles from lithographic processes: novel materials for fundamental and applied colloid science. *Curr. Opin. Colloid Interface Sci* 16, 106–117 (2011). [PubMed: 21516212]
56. Lee SA, Chung SE, Park W, Lee SH & Kwon S Three-dimensional fabrication of heterogeneous microstructures using soft membrane deformation and optofluidic maskless lithography. *Lab Chip* 9, 1670–1675 (2009). [PubMed: 19495448]
57. Chung SE, Park W, Shin S, Lee SA & Kwon S Guided and fluidic self-assembly of microstructures using railed microfluidic channels. *Nat. Mater* 7, 581–587 (2008). [PubMed: 18552850]
58. Nichol JW et al. Cell-laden microengineered gelatin methacrylate hydrogels. *Biomaterials* 31, 5536–5544 (2010). [PubMed: 20417964]
59. Panda P et al. Stop-flow lithography to generate cell-laden microgel particles. *Lab Chip* 8, 1056–1061 (2008). [PubMed: 18584079]
60. Jang J-H, Dendukuri D, Hatton TA, Thomas EL & Doyle PS A route to three-dimensional structures in a microfluidic device: stop-flow interference lithography. *Angew. Chem. Int. Ed* 119, 9185–9189 (2007).
61. Dendukuri D, Pregibon DC, Collins J, Hatton TA & Doyle PS Continuous-flow lithography for high-throughput microparticle synthesis. *Nat. Mater* 5, 365–369 (2006). [PubMed: 16604080]
62. Rolland JP et al. Direct fabrication and harvesting of monodisperse, shape-specific nanobiomaterials. *J. Am. Chem. Soc* 127, 10096–10100 (2005). [PubMed: 16011375]
63. Nielson R, Kaehr B & Shear JB Microreplication and design of biological architectures using dynamic-mask multiphoton lithography. *Small* 5, 120–125 (2009). [PubMed: 19040218]
64. Laza SC et al. Two-photon continuous flow lithography. *Adv. Mater* 24, 1304–1308 (2012). [PubMed: 22302705]
65. Dendukuri D, Gu SS, Pregibon DC, Hatton TA & Doyle PS Stop-flow lithography in a microfluidic device. *Lab Chip* 7, 818–828 (2007). [PubMed: 17593999]
66. Merkel TJ et al. The effect of particle size on the biodistribution of low-modulus hydrogel PRINT particles. *J. Control. Release* 162, 37–44 (2012). [PubMed: 22705460]
67. Khademhosseini A et al. Micromolding of photocrosslinkable hyaluronic acid for cell encapsulation and entrapment. *J. Biomed. Mater. Res. A* 79, 522–532 (2006). [PubMed: 16788972]
68. Baudis S et al. Modular material system for the microfabrication of biocompatible hydrogels based on thiol–ene-modified poly(vinyl alcohol). *J. Polym. Sci. Part A Polym. Chem* 54, 2060–2070 (2016).
69. Qin X-H et al. Enzymatic synthesis of hyaluronic acid vinyl esters for two-photon microfabrication of biocompatible and biodegradable hydrogel constructs. *Polym. Chem* 5, 6523–6533 (2014).
70. Gramlich WM, Kim IL & Burdick JA Synthesis and orthogonal photopatterning of hyaluronic acid hydrogels with thiol-norbornene chemistry. *Biomaterials* 34, 9803–9811 (2013). [PubMed: 24060422]
71. Ifkovits JL & Burdick JA Review: photopolymerizable and degradable biomaterials for tissue engineering applications. *Tissue Eng* 13, 2369–2385 (2007). [PubMed: 17658993]
72. Nguyen KT & West JL Photopolymerizable hydrogels for tissue engineering applications. *Biomaterials* 23, 4307–4314 (2002). [PubMed: 12219820]



73. Bahney CS et al. Visible light photoinitiation of mesenchymal stem cell-laden bioresponsive hydrogels. *Eur. Cell Mater* 22, 43–55 (2011). [PubMed: 21761391]
74. Bryant SJ, Nuttelman CR & Anseth KS Cytocompatibility of UV and visible light photoinitiating systems on cultured NIH/3T3 fibroblasts in vitro. *J. Biomater. Sci. Polym. Ed* 11, 439–457 (2000). [PubMed: 10896041]
75. Le Goff GC, Lee J, Gupta A, Hill WA & Doyle PS High-throughput contact flow lithography. *Adv. Sci* 2, 1500149 (2015).
76. Naqvi SM et al. Living cell factories - electrosprayed microcapsules and microcarriers for minimally invasive delivery. *Adv. Mater* 28, 5662–5671 (2016). [PubMed: 26695531]
77. Gansau J, Kelly L & Buckley CT Influence of key processing parameters and seeding density effects of microencapsulated chondrocytes fabricated using electrohydrodynamic spraying. *Biofabrication* 10, 035011 (2018). [PubMed: 29888707]
78. Pancholi K, Ahras N, Stride E & Edirisinghe M Novel electrohydrodynamic preparation of porous chitosan particles for drug delivery. *J. Mater. Sci. Mater. Med* 20, 917–923 (2009). [PubMed: 19034624]
79. Qayyum AS et al. Design of electrohydrodynamic sprayed polyethylene glycol hydrogel microspheres for cell encapsulation. *Biofabrication* 9, 025019 (2017). [PubMed: 28516893]
80. Young CJ, Poole-Warren LA & Martens PJ Combining submerged electrospray and UV photopolymerization for production of synthetic hydrogel microspheres for cell encapsulation. *Biotechnol. Bioeng* 109, 1561–1570 (2012). [PubMed: 22234803]
81. Kim PH et al. Injectable multifunctional microgel encapsulating outgrowth endothelial cells and growth factors for enhanced neovascularization. *J. Control. Release* 187, 1–13 (2014). [PubMed: 24852096]
82. Gu Z et al. Glucose-responsive microgels integrated with enzyme nanocapsules for closed-loop insulin delivery. *ACS Nano* 7, 6758–6766 (2013). [PubMed: 23834678]
83. Jayasinghe SN & Townsend-Nicholson A Stable electric-field driven cone-jetting of concentrated biosuspensions. *Lab Chip* 6, 1086–1090 (2006). [PubMed: 16874383]
84. Jayasinghe SN, Qureshi AN & Eagles PA Electrohydrodynamic jet processing: an advanced electric-field-driven jetting phenomenon for processing living cells. *Small* 2, 216–219 (2006). [PubMed: 17193023]
85. Sinclair A et al. Self-healing zwitterionic microgels as a versatile platform for malleable cell constructs and injectable therapies. *Adv. Mater* 30, 1803087 (2018).
86. Hinton TJ et al. Three-dimensional printing of complex biological structures by freeform reversible embedding of suspended hydrogels. *Science Adv* 1, e1500758 (2015).
87. Riley L, Schirmer L & Segura T Granular hydrogels: emergent properties of jammed hydrogel microparticles and their applications in tissue repair and regeneration. *Curr. Opin. Biotechnol* 60, 1–8 (2018). [PubMed: 30481603]
88. Behringer RP & Chakraborty B The physics of jamming for granular materials: a review. *Rep. Prog. Phys* 82, 012601 (2019). [PubMed: 30132446]
89. Hurley RC, Hall SA, Andrade JE & Wright J Quantifying interparticle forces and heterogeneity in 3D granular materials. *Phys. Rev. Lett* 117, 098005 (2016). [PubMed: 27610890]
90. Weeks ER in *Statistical physics of complex fluids* (eds Maruyama S & Tokuyama M) 1–53 (Tohoku University Press, 2007).
91. Torquato S & Stillinger FH Jammed hard-particle packings: From Kepler to Bernal and beyond. *Rev. Mod. Phys* 82, 2633–2672 (2010).
92. Menut P, Seiffert S, Sprakel J & Weitz DA Does size matter? Elasticity of compressed suspensions of colloidal- and granular-scale microgels. *Soft Matter* 8, 156–164 (2012).
93. Liu AJ & Nagel SR The jamming transition and the marginally jammed solid. *Annu. Rev. Condens. Matter Phys* 1, 347–369 (2010).
94. van Hecke M Jamming of soft particles: geometry, mechanics, scaling and isostaticity. *J. Phys. Condens. Matter* 22, 033101 (2009). [PubMed: 21386274]
95. Yuan Y, Liu L, Zhuang Y, Jin W & Li S Coupling effects of particle size and shape on improving the density of disordered polydisperse packings. *Phys. Rev. E* 98, 042903 (2018).



96. Hausteine M, Gladky A & Schwarze R Discrete element modeling of deformable particles in YADE. *SoftwareX* 6, 118–123 (2017).
97. Sun Q, Jin F, Liu J & Zhang G Understanding force chains in dense granular materials. *Int. J. Mod. Phys. B* 24, 5743–5759 (2010).
98. Truong NF et al. Microporous annealed particle hydrogel stiffness, void space size, and adhesion properties impact cell proliferation, cell spreading, and gene transfer. *Acta Biomater* 94, 160–172 (2019). [PubMed: 31154058]
99. Kim J, Yaszemski MJ & Lu L Three-dimensional porous biodegradable polymeric scaffolds fabricated with biodegradable hydrogel porogens. *Tissue Eng. Part C Methods* 15, 583–594 (2009). [PubMed: 19216632]
100. Wang L, Lu S, Lam J, Kasper FK & Mikos AG Fabrication of cell-laden macroporous biodegradable hydrogels with tunable porosities and pore sizes. *Tissue Eng. Part C Methods* 21, 263–273 (2014). [PubMed: 25156274]
101. Hu J et al. Microgel-reinforced hydrogel films with high mechanical strength and their visible mesoscale fracture structure. *Macromolecules* 44, 7775–7781 (2011).
102. Shin H, Olsen BD & Khademhosseini A Gellan gum microgel-reinforced cell-laden gelatin hydrogels. *J. Mater. Chem. B* 2, 2508–2516 (2014). [PubMed: 25309744]
103. Nih LR, Sideris E, Carmichael ST & Segura T Injection of microporous annealing particle (MAP) hydrogels in the stroke cavity reduces gliosis and inflammation and promotes NPC migration to the lesion. *Adv. Mater* 29, 1606471 (2017).
104. Darling NJ, Sideris E, Hamada N, Carmichael ST & Segura T Injectable and spatially patterned microporous annealed particle (MAP) hydrogels for tissue repair applications. *Adv. Sci* 5, 1801046 (2018).
105. Le LV et al. Injectable hyaluronic acid based microrods provide local micromechanical and biochemical cues to attenuate cardiac fibrosis after myocardial infarction. *Biomaterials* 169, 11–21 (2018). [PubMed: 29631164]
106. Caldwell AS, Campbell GT, Shekiri KMT & Anseth KS Clickable microgel scaffolds as platforms for 3D cell encapsulation. *Adv. Healthc. Mater* 6, 1700254 (2017).
107. Madl CM, Heilshorn SC & Blau HM Bioengineering strategies to accelerate stem cell therapeutics. *Nature* 557, 335–342 (2018). [PubMed: 29769665]
108. Seliktar D Designing cell-compatible hydrogels for biomedical applications. *Science* 336, 1124–1128 (2012). [PubMed: 22654050]
109. Wang C, Varshney RR & Wang D-A Therapeutic cell delivery and fate control in hydrogels and hydrogel hybrids. *Adv. Drug Deliv. Rev* 62, 699–710 (2010). [PubMed: 20138940]
110. Rosales AM & Anseth KS The design of reversible hydrogels to capture extracellular matrix dynamics. *Nat. Rev. Mater* 1, 15012 (2016). [PubMed: 29214058]
111. Prince E & Kumacheva E Design and applications of man-made biomimetic fibrillar hydrogels. *Nat. Rev. Mater* 4, 99–115 (2019).
112. Mao AS et al. Deterministic encapsulation of single cells in thin tunable microgels for niche modelling and therapeutic delivery. *Nat. Mater* 16, 236–243 (2016). [PubMed: 27798621]
113. Daly AC, Sathy BN & Kelly DJ Engineering large cartilage tissues using dynamic bioreactor culture at defined oxygen conditions. *J. Tissue Eng* 9, 2041731417753718 (2018). [PubMed: 29399319]
114. Sheehy EJ, Buckley CT & Kelly DJ Chondrocytes and bone marrow-derived mesenchymal stem cells undergoing chondrogenesis in agarose hydrogels of solid and channelled architectures respond differentially to dynamic culture conditions. *J. Tissue Eng. Regen. Med* 5, 747–758 (2011). [PubMed: 21953872]
115. Daly AC & Kelly DJ Biofabrication of spatially organised tissues by directing the growth of cellular spheroids within 3D printed polymeric microchambers. *Biomaterials* 197, 194–206 (2019). [PubMed: 30660995]
116. Kolesky DB, Homan KA, Skylar-Scott MA & Lewis JA Three-dimensional bioprinting of thick vascularized tissues. *Proc. Natl. Acad. Sci. USA* 113, 3179–3184 (2016). [PubMed: 26951646]
117. Madl CM & Heilshorn SC Engineering hydrogel microenvironments to recapitulate the stem cell niche. *Annu. Rev. Biomed. Eng* 20, 21–47 (2018). [PubMed: 29220201]

118. Rapp TL, Highley CB, Manor BC, Burdick JA & Dmochowski IJ Ruthenium-crosslinked hydrogels with rapid, visible-light degradation. *Chem* 24, 2328–2333 (2018).
119. Mohamed MGA et al. An integrated microfluidic flow-focusing platform for on-chip fabrication and filtration of cell-laden microgels. *Lab Chip* 19, 1621–1632 (2019). [PubMed: 30896015]
120. Deng Y et al. Rapid purification of cell encapsulated hydrogel beads from oil phase to aqueous phase in a microfluidic device. *Lab Chip* 11, 4117–4121 (2011). [PubMed: 22012540]
121. Choi CH et al. One-step generation of cell-laden microgels using double emulsion drops with a sacrificial ultra-thin oil shell. *Lab Chip* 16, 1549–1555 (2016). [PubMed: 27070224]
122. Zhu K et al. All-aqueous-phase microfluidics for cell encapsulation. *ACS Appl. Mater. Interfaces* 11, 4826–4832 (2019). [PubMed: 30648845]
123. Maeda K, Onoe H, Takinoue M & Takeuchi S Controlled synthesis of 3D multi-compartmental particles with centrifuge-based microdroplet formation from a multi-barrelled capillary. *Adv. Mater* 24, 1340–1346 (2012). [PubMed: 22311473]
124. Ma C, Tian C, Zhao L & Wang J Pneumatic-aided micro-molding for flexible fabrication of homogeneous and heterogeneous cell-laden microgels. *Lab Chip* 16, 2609–2617 (2016). [PubMed: 27229899]
125. Allazetta S, Kolb L, Zerbib S, Bardy J & Lutolf MP Cell-instructive microgels with tailor-made physicochemical properties. *Small* 11, 5647–5656 (2015). [PubMed: 26349486]
126. Blaeser A et al. Controlling shear stress in 3D bioprinting is a key factor to balance printing resolution and stem cell integrity. *Adv. Healthc. Mater* 5, 326–333 (2016). [PubMed: 26626828]
127. Chen MH et al. Methods to assess shear-thinning hydrogels for application as injectable biomaterials. *ACS Biomater. Sci. Eng* 3, 3146–3160 (2017). [PubMed: 29250593]
128. Aguado BA, Mulyasmita W, Su J, Lampe KJ & Heilshorn SC Improving viability of stem cells during syringe needle flow through the design of hydrogel cell carriers. *Tissue Eng. Part A* 18, 806–815 (2011). [PubMed: 22011213]
129. Zhao X et al. Injectable stem cell-laden photocrosslinkable microspheres fabricated using microfluidics for rapid generation of osteogenic tissue constructs. *Adv. Funct. Mater* 26, 2809–2819 (2016).
130. Annamalai RT et al. Injectable osteogenic microtissues containing mesenchymal stromal cells conformally fill and repair critical-size defects. *Biomaterials* 208, 32–44 (2019). [PubMed: 30991216]
131. Wise JK, Alford AI, Goldstein SA & Stegemann JP Synergistic enhancement of ectopic bone formation by supplementation of freshly isolated marrow cells with purified MSC in collagen–chitosan hydrogel microbeads. *Connect. Tissue Res* 57, 516–525 (2016). [PubMed: 26337827]
132. Wang L, Rao RR & Stegemann JP Delivery of mesenchymal stem cells in chitosan/collagen microbeads for orthopedic tissue repair. *Cells Tissues Organs* 197, 333–343 (2013). [PubMed: 23571151]
133. Daley ELH, Coleman RM & Stegemann JP Biomimetic microbeads containing a chondroitin sulfate/chitosan polyelectrolyte complex for cell-based cartilage therapy. *J. Mater. Chem. B* 3, 7920–7929 (2015). [PubMed: 26693016]
134. Li F et al. Cartilage tissue formation through assembly of microgels containing mesenchymal stem cells. *Acta Biomater* 77, 48–62 (2018). [PubMed: 30006317]
135. Yin H et al. Functional tissue-engineered microtissue derived from cartilage extracellular matrix for articular cartilage regeneration. *Acta Biomater* 77, 127–141 (2018). [PubMed: 30030172]
136. Wang Y et al. Fabrication of nanofibrous microcarriers mimicking extracellular matrix for functional microtissue formation and cartilage regeneration. *Biomaterials* 171, 118–132 (2018). [PubMed: 29684676]
137. Feyen DAM et al. Gelatin microspheres as vehicle for cardiac progenitor cells delivery to the myocardium. *Adv. Healthc. Mater* 5, 1071–1079 (2016). [PubMed: 26913710]
138. Shrestha P, Regmi S & Jeong J-H Injectable hydrogels for islet transplantation: a concise review. *Int. J. Pharm. Investig* 1–17 (2019).
139. Veiseth O et al. Size- and shape-dependent foreign body immune response to materials implanted in rodents and non-human primates. *Nat. Mater* 14, 643–651 (2015). [PubMed: 25985456]

140. Headen DM et al. Local immunomodulation with Fas ligand-engineered biomaterials achieves allogeneic islet graft acceptance. *Nat. Mater* 17, 732–739 (2018). [PubMed: 29867165]
141. Hoare TR & Kohane DS Hydrogels in drug delivery: Progress and challenges. *Polymer* 49, 1993–2007 (2008).
142. Guvendiren M, Lu HD & Burdick JA Shear-thinning hydrogels for biomedical applications. *Soft Matter* 8, 260–272 (2012).
143. Dimatteo R, Darling NJ & Segura T In situ forming injectable hydrogels for drug delivery and wound repair. *Adv. Drug Deliv. Rev* 127, 167–184 (2018). [PubMed: 29567395]
144. Chen W, Palazzo A, Hennink WE & Kok RJ Effect of particle size on drug loading and release kinetics of gefitinib-loaded PLGA microspheres. *Mol. Pharm* 14, 459–467 (2017). [PubMed: 27973854]
145. Freiberg S & Zhu XX Polymer microspheres for controlled drug release. *Int. J. Pharm* 282, 1–18 (2004). [PubMed: 15336378]
146. Nguyen AH, McKinney J, Miller T, Bongiorno T & McDevitt TC Gelatin methacrylate microspheres for controlled growth factor release. *Acta Biomater* 13, 101–110 (2015). [PubMed: 25463489]
147. Solorio LD, Dhami CD, Dang PN, Vieregge EL & Alsberg E Spatiotemporal regulation of chondrogenic differentiation with controlled delivery of transforming growth factor- $\beta$ 1 from gelatin microspheres in mesenchymal stem cell aggregates. *Stem Cells Transl. Med* 1, 632–639 (2012). [PubMed: 23197869]
148. Censi R, Di Martino P, Vermonden T & Hennink WE Hydrogels for protein delivery in tissue engineering. *J. Control. Release* 161, 680–692 (2012). [PubMed: 22421425]
149. Hettiaratchi MH, Miller T, Temenoff JS, Guldberg RE & McDevitt TC Heparin microparticle effects on presentation and bioactivity of bone morphogenetic protein-2. *Biomaterials* 35, 7228–7238 (2014). [PubMed: 24881028]
150. Feng Q et al. Sulfated hyaluronic acid hydrogels with retarded degradation and enhanced growth factor retention promote hMSC chondrogenesis and articular cartilage integrity with reduced hypertrophy. *Acta Biomater* 53, 329–342 (2017). [PubMed: 28193542]
151. Öztürk E et al. Sulfated hydrogel matrices direct mitogenicity and maintenance of chondrocyte phenotype through activation of FGF signaling. *Adv. Funct. Mater* 26, 3649–3662 (2016). [PubMed: 28919847]
152. Freeman I, Kedem A & Cohen S The effect of sulfation of alginate hydrogels on the specific binding and controlled release of heparin-binding proteins. *Biomaterials* 29, 3260–3268 (2008). [PubMed: 18462788]
153. Buket Basmanav F, Kose GT & Hasirci V Sequential growth factor delivery from complexed microspheres for bone tissue engineering. *Biomaterials* 29, 4195–4204 (2008). [PubMed: 18691753]
154. Jaklenec A et al. Sequential release of bioactive IGF-I and TGF- $\beta$ 1 from PLGA microsphere-based scaffolds. *Biomaterials* 29, 1518–1525 (2008). [PubMed: 18166223]
155. Wang Y, Cooke MJ, Sachewsky N, Morshead CM & Shoichet MS Bioengineered sequential growth factor delivery stimulates brain tissue regeneration after stroke. *J. Control. Release* 172, 1–11 (2013). [PubMed: 23933523]
156. McGillicuddy FC et al. Novel “plum pudding” gels as potential drug-eluting stent coatings: controlled release of fluvastatin. *J. Biomed. Mater. Res. A* 79, 923–933 (2006). [PubMed: 16941598]
157. Sivakumaran D, Maitland D & Hoare T Injectable microgel-hydrogel composites for prolonged small-molecule drug delivery. *Biomacromolecules* 12, 4112–4120 (2011). [PubMed: 22007750]
158. Almeida HV et al. Controlled release of transforming growth factor- $\beta$ 3 from cartilage-extra-cellular-matrix-derived scaffolds to promote chondrogenesis of human-joint-tissue-derived stem cells. *Acta Biomater* 10, 4400–4409 (2014). [PubMed: 24907658]
159. Bian L et al. Enhanced MSC chondrogenesis following delivery of TGF- $\beta$ 3 from alginate microspheres within hyaluronic acid hydrogels in vitro and in vivo. *Biomaterials* 32, 6425–6434 (2011). [PubMed: 21652067]

160. Patel ZS, Yamamoto M, Ueda H, Tabata Y & Mikos AG Biodegradable gelatin microparticles as delivery systems for the controlled release of bone morphogenetic protein-2. *Acta Biomater* 4, 1126–1138 (2008). [PubMed: 18474452]
161. Kavanaugh TE, Werfel TA, Cho H, Hasty KA & Duvall CL Particle-based technologies for osteoarthritis detection and therapy. *Drug Deliv. Transl. Res* 6, 132–147 (2016). [PubMed: 25990835]
162. Li M, Liu X, Liu X & Ge B Calcium phosphate cement with BMP-2-loaded gelatin microspheres enhances bone healing in osteoporosis: a pilot study. *Clin. Orthop. Relat. Res* 468, 1978–1985 (2010). [PubMed: 20306162]
163. Patel ZS et al. Dual delivery of an angiogenic and an osteogenic growth factor for bone regeneration in a critical size defect model. *Bone* 43, 931–940 (2008). [PubMed: 18675385]
164. Cai B et al. Injectable gel constructs with regenerative and anti-infective dual effects based on assembled chitosan microspheres. *ACS Appl. Mater. Interfaces* 10, 25099–25112 (2018). [PubMed: 29952200]
165. DeFail AJ, Chu CR, Izzo N & Marra KG Controlled release of bioactive TGF- $\beta$ 1 from microspheres embedded within biodegradable hydrogels. *Biomaterials* 27, 1579–1585 (2006). [PubMed: 16140372]
166. Holland TA, Tabata Y & Mikos AG Dual growth factor delivery from degradable oligo(poly(ethylene glycol) fumarate) hydrogel scaffolds for cartilage tissue engineering. *J. Control. Release* 101, 111–125 (2005). [PubMed: 15588898]
167. Park H, Temenoff JS, Holland TA, Tabata Y & Mikos AG Delivery of TGF- $\beta$ 1 and chondrocytes via injectable, biodegradable hydrogels for cartilage tissue engineering applications. *Biomaterials* 26, 7095–7103 (2005). [PubMed: 16023196]
168. Kang ML, Ko J-Y, Kim JE & Im G-I Intra-articular delivery of kartogenin-conjugated chitosan nano/microparticles for cartilage regeneration. *Biomaterials* 35, 9984–9994 (2014). [PubMed: 25241157]
169. Hoshino K et al. Three catheter-based strategies for cardiac delivery of therapeutic gelatin microspheres. *Gene Ther* 13, 1320–1327 (2006). [PubMed: 16708077]
170. Iwakura A et al. Intramyocardial sustained delivery of basic fibroblast growth factor improves angiogenesis and ventricular function in a rat infarct model. *Heart Vessels* 18, 93–99 (2003). [PubMed: 12756606]
171. Liu Y, Sun L, Huan Y, Zhao H & Deng J Effects of basic fibroblast growth factor microspheres on angiogenesis in ischemic myocardium and cardiac function: analysis with dobutamine cardiovascular magnetic resonance tagging. *Eur. J. Cardiothorac. Surg* 30, 103–107 (2006). [PubMed: 16730451]
172. Uitterdijk A et al. VEGF165A microsphere therapy for myocardial infarction suppresses acute cytokine release and increases microvascular density but does not improve cardiac function. *Am. J. Physiol. Heart Circ. Physiol* 309, H396–H406 (2015). [PubMed: 26024685]
173. Chen MH et al. Injectable supramolecular hydrogel/microgel composites for therapeutic delivery. *Macromol. Biosci* 19, e1800248 (2019). [PubMed: 30259658]
174. Du J, Du P & Smyth HD Hydrogels for controlled pulmonary delivery. *Ther. Deliv* 4, 1293–1305 (2013). [PubMed: 24116913]
175. ul-Ain Qurrat, Sharma S, Khuller GK & Garg SK Alginate-based oral drug delivery system for tuberculosis: pharmacokinetics and therapeutic effects. *J. Antimicrob. Chemother* 51, 931–938 (2003). [PubMed: 12654730]
176. Selvam P, El-Sherbiny IM & Smyth HD Swellable hydrogel particles for controlled release pulmonary administration using propellant-driven metered dose inhalers. *J. Aerosol. Med. Pulm. Drug Deliv* 24, 25–34 (2011). [PubMed: 20961166]
177. El-Sherbiny IM, McGill S & Smyth HD Swellable microparticles as carriers for sustained pulmonary drug delivery. *J. Pharm. Sci* 99, 2343–2356 (2010). [PubMed: 19967777]
178. Hwang SM, Kim DD, Chung SJ & Shim CK Delivery of ofloxacin to the lung and alveolar macrophages via hyaluronan microspheres for the treatment of tuberculosis. *J. Control. Release* 129, 100–106 (2008). [PubMed: 18538437]

179. Secret E, Crannell KE, Kelly SJ, Villancio-Wolter M & Andrew JS Matrix metalloproteinase-sensitive hydrogel microparticles for pulmonary drug delivery of small molecule drugs or proteins. *J. Mater. Chem. B* 3, 5629–5634 (2015). [PubMed: 32262533]
180. Secret E, Kelly SJ, Crannell KE & Andrew JS Enzyme-responsive hydrogel microparticles for pulmonary drug delivery. *ACS Appl. Mater. Interfaces* 6, 10313–10321 (2014). [PubMed: 24926532]
181. Chaturvedi K, Ganguly K, Nadagouda MN & Aminabhavi TM Polymeric hydrogels for oral insulin delivery. *J. Control. Release* 165, 129–138 (2013). [PubMed: 23159827]
182. Bell CL & Peppas NA Water, solute and protein diffusion in physiologically responsive hydrogels of poly(methacrylic acid-g-ethylene glycol). *Biomaterials* 17, 1203–1218 (1996). [PubMed: 8799505]
183. Mundargi RC, Rangaswamy V & Aminabhavi TM Poly(N-vinylcaprolactam-co-methacrylic acid) hydrogel microparticles for oral insulin delivery. *J. Microencapsul* 28, 384–394 (2011). [PubMed: 21736523]
184. Sajeesh S, Bouchemal K, Marsaud V, Vauthier C & Sharma CP Cyclodextrin complexed insulin encapsulated hydrogel microparticles: An oral delivery system for insulin. *J. Control. Release* 147, 377–384 (2010). [PubMed: 20727924]
185. Bravo-Osuna I, Vauthier C, Farabollini A, Palmieri GF & Ponchel G Mucoadhesion mechanism of chitosan and thiolated chitosan-poly(isobutyl cyanoacrylate) core-shell nanoparticles. *Biomaterials* 28, 2233–2243 (2007). [PubMed: 17261330]
186. Zhang Y, Wei W, Lv P, Wang L & Ma G Preparation and evaluation of alginate–chitosan microspheres for oral delivery of insulin. *Eur. J. Pharm. Biopharm* 77, 11–19 (2011). [PubMed: 20933083]
187. He P, Davis SS & Illum L In vitro evaluation of the mucoadhesive properties of chitosan microspheres. *Int. J. Pharm* 166, 75–88 (1998).
188. Solorio LD, Fu AS, Hernández-Irizarry R & Alsberg E Chondrogenic differentiation of human mesenchymal stem cell aggregates via controlled release of TGF- $\beta$ 1 from incorporated polymer microspheres. *J. Biomed. Mater. Res. A* 92A, 1139–1144 (2010).
189. Solorio LD, Vieregge EL, Dhami CD, Dang PN & Alsberg E Engineered cartilage via self-assembled hMSC sheets with incorporated biodegradable gelatin microspheres releasing transforming growth factor- $\beta$ 1. *J. Control. Release* 158, 224–232 (2012). [PubMed: 22100386]
190. Bratt-Leal AM, Nguyen AH, Hammersmith KA, Singh A & McDevitt TC A microparticle approach to morphogen delivery within pluripotent stem cell aggregates. *Biomaterials* 34, 7227–7235 (2013). [PubMed: 23827184]
191. Collins MN & Birkinshaw C Hyaluronic acid based scaffolds for tissue engineering—A review. *Carbohydr. Polym* 92, 1262–1279 (2013). [PubMed: 23399155]
192. Chan BP & Leong KW Scaffolding in tissue engineering: general approaches and tissue-specific considerations. *Eur. Spine J* 17, 467–479 (2008). [PubMed: 19005702]
193. Ahmed EM Hydrogel: Preparation, characterization, and applications: A review. *J. Adv. Res* 6, 105–121 (2015). [PubMed: 25750745]
194. Sheikh A et al. Microfluidic-enabled bottom-up hydrogels from annealable naturally-derived protein microbeads. *Biomaterials* 192, 560–568 (2019). [PubMed: 30530245]
195. Xin S, Wyman OM & Alge DL Assembly of PEG microgels into porous cell-instructive 3D scaffolds via thiol-ene click chemistry. *Adv. Healthc. Mater* 7, e1800160 (2018). [PubMed: 29663702]
196. Hsu RS et al. Adaptable microporous hydrogels of propagating NGF-gradient by injectable building blocks for accelerated axonal outgrowth. *Adv. Sci* 6, 1900520 (2019).
197. McWhorter FY, Wang T, Nguyen P, Chung T & Liu WF Modulation of macrophage phenotype by cell shape. *Proc. Natl. Acad. Sci. USA* 110, 17253–17258 (2013). [PubMed: 24101477]
198. Werner M et al. Surface curvature differentially regulates stem cell migration and differentiation via altered attachment morphology and nuclear deformation. *Adv. Sci* 4, 1600347 (2017).
199. Mitra A et al. Cell geometry dictates TNF $\alpha$ -induced genome response. *Proc. Natl. Acad. Sci. USA* 114, E3882–E3891 (2017). [PubMed: 28461498]



200. Li S et al. Hydrogels with precisely controlled integrin activation dictate vascular patterning and permeability. *Nat. Mater* 16, 953–961 (2017). [PubMed: 28783156]
201. Bae M-S, Lee KY, Park YJ & Mooney DJ RGD island spacing controls phenotype of primary human fibroblasts adhered to ligand-organized hydrogels. *Macromol. Res* 15, 469–472 (2007).
202. Cruz DM et al. Chitosan microparticles as injectable scaffolds for tissue engineering. *J. Tissue Eng. Regen. Med* 2, 378–380 (2008). [PubMed: 18615778]
203. Malafaya PB, Santos TC, van Griensven M & Reis RL Morphology, mechanical characterization and in vivo neo-vascularization of chitosan particle aggregated scaffolds architectures. *Biomaterials* 29, 3914–3926 (2008). [PubMed: 18649938]
204. Kucharska M et al. Fabrication and characterization of chitosan microspheres agglomerated scaffolds for bone tissue engineering. *Mater. Lett* 64, 1059–1062 (2010).
205. Dumont CM et al. Aligned hydrogel tubes guide regeneration following spinal cord injury. *Acta Biomater* 86, 312–322 (2019). [PubMed: 30610918]
206. Hu Z, Ma C, Rong X, Zou S & Liu X Immunomodulatory ECM-like microspheres for accelerated bone regeneration in diabetes mellitus. *ACS Appl. Mater. Interfaces* 10, 2377–2390 (2018). [PubMed: 29280610]
207. Roam JL, Nguyen PK & Elbert DL Controlled release and gradient formation of human glial-cell derived neurotrophic factor from heparinated poly(ethylene glycol) microsphere-based scaffolds. *Biomaterials* 35, 6473–6481 (2014). [PubMed: 24816282]
208. Roam JL et al. A modular, plasmin-sensitive, clickable poly(ethylene glycol)-heparin-laminin microsphere system for establishing growth factor gradients in nerve guidance conduits. *Biomaterials* 72, 112–124 (2015). [PubMed: 26352518]
209. Custódio CA et al. Functionalized microparticles producing scaffolds in combination with cells. *Adv. Funct. Mater* 24, 1391–1400 (2014).
210. Jgamadze D, Liu L, Vogler S, Chu LY & Pautot S Thermoswitching microgel carriers improve neuronal cell growth and cell release for cell transplantation. *Tissue Eng. C Methods* 21, 65–76 (2015).
211. Moroni L et al. Biofabrication strategies for 3D in vitro models and regenerative medicine. *Nat. Rev. Mater* 3, 21–37 (2018). [PubMed: 31223488]
212. Groll J et al. Biofabrication: reappraising the definition of an evolving field. *Biofabrication* 8, 013001 (2016). [PubMed: 26744832]
213. Xu F et al. Three-dimensional magnetic assembly of microscale hydrogels. *Adv. Mater* 23, 4254–4260 (2011). [PubMed: 21830240]
214. Tasoglu S, Diller E, Guven S, Sitti M & Demirci U Untethered micro-robotic coding of three-dimensional material composition. *Nat. Commun* 5, 3124 (2014). [PubMed: 24469115]
215. Xu F et al. The assembly of cell-encapsulating microscale hydrogels using acoustic waves. *Biomaterials* 32, 7847–7855 (2011). [PubMed: 21820734]
216. Kamperman T et al. Single cell microgel based modular bioinks for uncoupled cellular micro- and macroenvironments. *Adv. Healthc. Mater* 6, 1600913 (2017).
217. Xin S, Chimene D, Garza JE, Gaharwar AK & Alge DL Clickable PEG hydrogel microspheres as building blocks for 3D bioprinting. *Biomater. Sci* 7, 1179–1187 (2019). [PubMed: 30656307]
218. Highley CB, Rodell CB & Burdick JA Direct 3D printing of shear-thinning hydrogels into self-healing hydrogels. *Adv. Mater* 27, 5075–5079 (2015). [PubMed: 26177925]
219. Bhattacharjee T et al. Writing in the granular gel medium. *Sci. Adv* 1, e1500655 (2015). [PubMed: 26601274]
220. Bhattacharjee T et al. Liquid-like solids support cells in 3D. *ACS Biomater. Sci. Eng* 2, 1787–1795 (2016). [PubMed: 33440476]
221. Gilbert E, Hui A & Waldorf HA The basic science of dermal fillers: past and present part I: background and mechanisms of action. *J. Drugs Dermatol* 11, 1059–1068 (2012). [PubMed: 23135648]
222. Tezel A & Fredrickson GH The science of hyaluronic acid dermal fillers. *J. Cosmet. Laser Ther* 10, 35–42 (2008). [PubMed: 18330796]



223. Rose JC et al. Nerve cells decide to orient inside an injectable hydrogel with minimal structural guidance. *Nano Lett* 17, 3782–3791 (2017). [PubMed: 28326790]
224. Le LV, Mkrtschjan MA, Russell B & Desai TA Hang on tight: reprogramming the cell with microstructural cues. *Biomed. Microdevices* 21, 43 (2019). [PubMed: 30955102]
225. Tan H et al. Heterogeneous multi-compartmental hydrogel particles as synthetic cells for incompatible tandem reactions. *Nat. Commun* 8, 663 (2017). [PubMed: 28939810]
226. Yadavali S, Jeong HH, Lee D & Issadore D Silicon and glass very large scale microfluidic droplet integration for terascale generation of polymer microparticles. *Nat. Commun* 9, 1222 (2018). [PubMed: 29581433]
227. Andrade JE, Avila CF, Hall SA, Lenoir N & Viggiani G Multiscale modeling and characterization of granular matter: from grain kinematics to continuum mechanics. *J. Mech. Phys. Solids* 59, 237–250 (2011).
228. Liu J, Bosco E & Suiker ASJ Multi-scale modelling of granular materials: numerical framework and study on micro-structural features. *Comput. Mech* 63, 409–427 (2019).
229. Zhu H et al. Spatial control of in vivo CRISPR–Cas9 genome editing via nanomagnets. *Nat. Biomed. Eng* 3, 126–136 (2019). [PubMed: 30944431]
230. Lu L, Stamatas GN & Mikos AG Controlled release of transforming growth factor  $\beta$ 1 from biodegradable polymer microparticles. *J. Biomed. Mater. Res* 50, 440–451 (2000). [PubMed: 10737887]
231. Pregibon DC, Toner M & Doyle PS Multifunctional encoded particles for high-throughput biomolecule analysis. *Science* 315, 1393–1396 (2007). [PubMed: 17347435]
232. Wang S et al. An in-situ photocrosslinking microfluidic technique to generate non-spherical, cytocompatible, degradable, monodisperse alginate microgels for chondrocyte encapsulation. *Biomicrofluidics* 12, 014106 (2018). [PubMed: 29375727]
233. Wang H et al. One-step generation of core–shell gelatin methacrylate (GelMA) microgels using a droplet microfluidic system. *Adv. Mater. Technol* 4, 1800632 (2019).
234. Jha AK, Malik MS, Farach-Carson MC, Duncan RL & Jia X Hierarchically structured, hyaluronic acid-based hydrogel matrices via the covalent integration of microgels into macroscopic networks. *Soft Matter* 6, 5045–5055 (2010). [PubMed: 20936090]
235. Loebel C, Broguiere N, Alini M, Zenobi-Wong M & Eglin D Microfabrication of photo-cross-linked hyaluronan hydrogels by single- and two-photon tyramine oxidation. *Biomacromolecules* 16, 2624–2630 (2015). [PubMed: 26222128]
236. Ma T, Gao X, Dong H, He H & Cao X High-throughput generation of hyaluronic acid microgels via microfluidics-assisted enzymatic crosslinking and/or Diels–Alder click chemistry for cell encapsulation and delivery. *Appl. Mater. Today* 9, 49–59 (2017).
237. Jia X et al. Hyaluronic acid-based microgels and microgel networks for vocal fold regeneration. *Biomacromolecules* 7, 3336–3344 (2006). [PubMed: 17154461]
238. Chen J et al. Tailor-making fluorescent hyaluronic acid microgels via combining microfluidics and photoclick chemistry for sustained and localized delivery of herceptin in tumors. *ACS Appl. Mater. Interfaces* 10, 3929–3937 (2018). [PubMed: 29302970]
239. Sonnet C et al. Rapid healing of femoral defects in rats with low dose sustained BMP2 expression from PEGDA hydrogel microspheres. *J. Orthop. Res* 31, 1597–1604 (2013). [PubMed: 23832813]
240. Chung SE et al. Optofluidic maskless lithography system for real-time synthesis of photopolymerized microstructures in microfluidic channels. *Appl. Phys. Lett* 91, 041106 (2007).
241. Ryu S et al. Dual mode gelation behavior of silk fibroin microgel embedded poly(ethylene glycol) hydrogels. *J. Mater. Chem. B* 4, 4574–4584 (2016). [PubMed: 32263400]
242. Kumachev A et al. High-throughput generation of hydrogel microbeads with varying elasticity for cell encapsulation. *Biomaterials* 32, 1477–1483 (2011). [PubMed: 21095000]

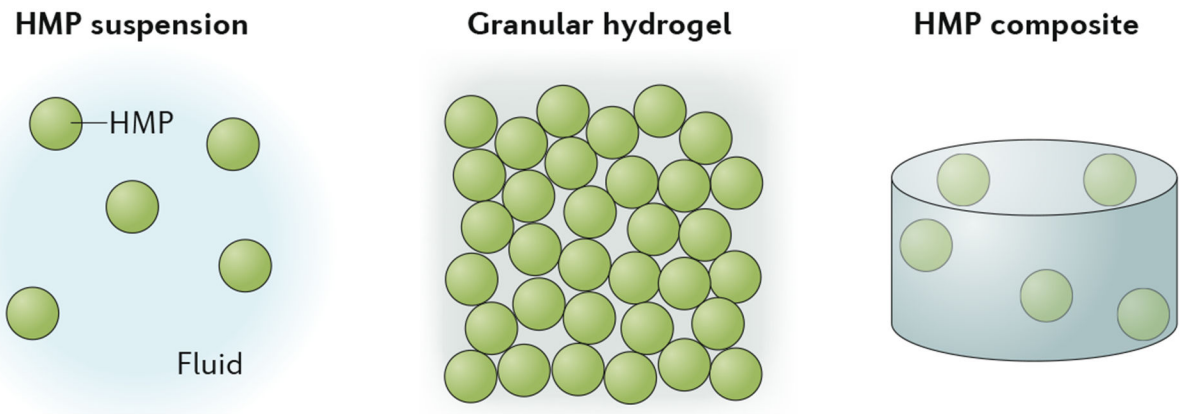


**Fig. 1 |. Categories of hydrogel microparticles.**

Hydrogel microparticles (HMPs) can be fabricated and used as distinct units or in aggregation. Their aggregates can be categorized as suspensions, granular hydrogels or composites if HMPs are embedded within a bulk hydrogel.

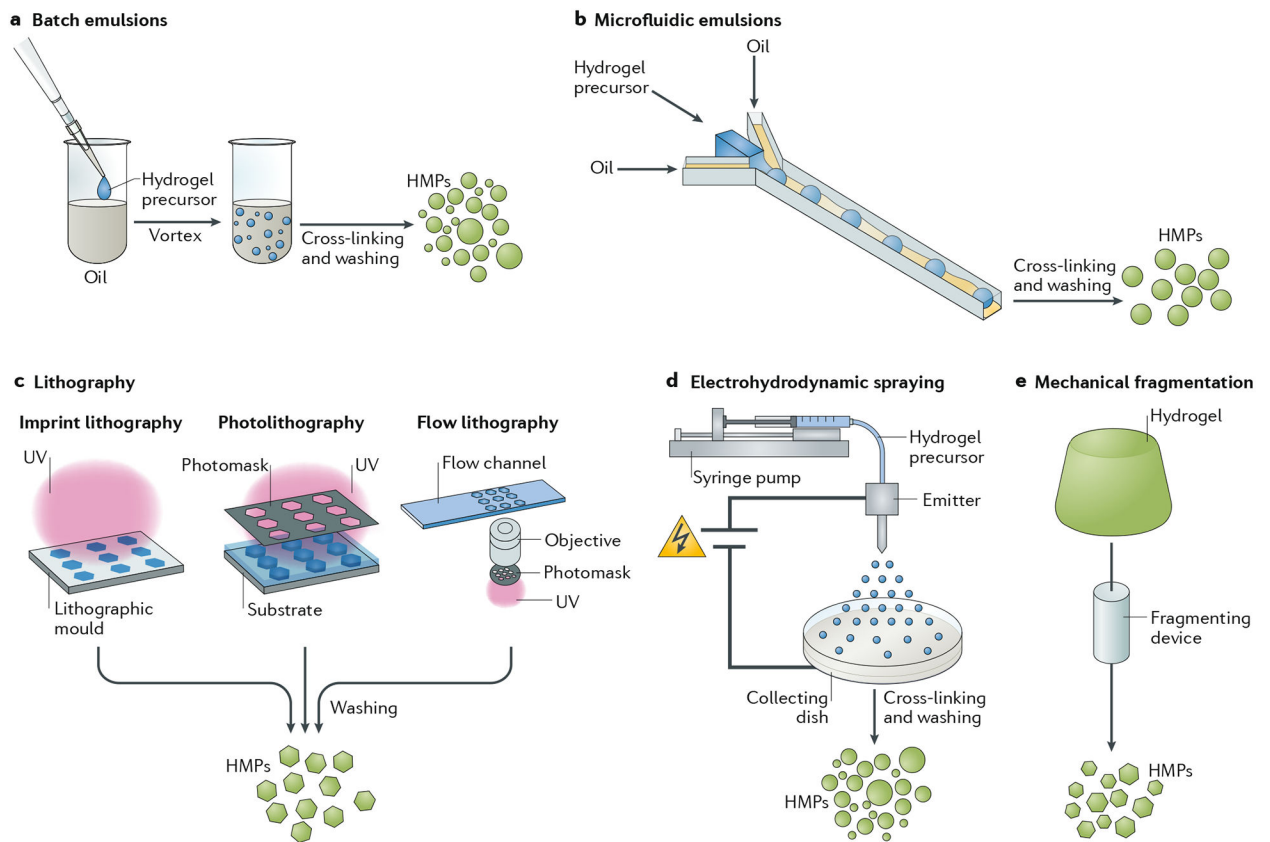


**Fig. 2 | Fabrication of hydrogel microparticles.**

Examples of fabrication techniques include: **a** | Batch emulsions, in which immiscible liquids are mixed together (for example, water and oil) to generate droplets that can be cross-linked to form hydrogel microparticles (HMPs). **b** | Microfluidic emulsions, in which flow-focusing junctions are used to generate droplets that can be subsequently cross-linked to form HMPs. **c** | Lithography, in which masks or moulds are used as templates for hydrogels at the microscale. **d** | Electrohydrodynamic spraying, in which electrical forces are used to charge flowing solutions to form droplets that can then be cross-linked into hydrogels. **e** | Mechanical fragmentation techniques, in which mechanical energy is used to fragment preformed hydrogels into smaller particles. Blue shading refers to uncross-linked solution, green shading refers to cross-linked HMPs or hydrogel. UV, ultraviolet.

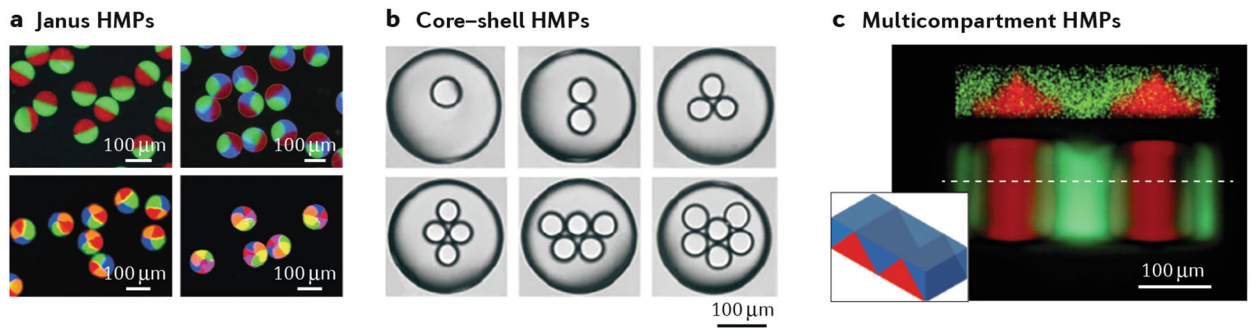


**Fig. 3 |. Microfluidic and lithographic templating of compartmentalized hydrogel microparticles.** **a** | Microfluidic formation of Janus (multiple-sided) hydrogel microparticles (HMPs) containing up to six distinct compartments, which is achieved by using multibarrel microcapillaries<sup>123</sup>. **b** | Formation of structured core-shell HMPs containing multiple compartments using co-axial, flow-focusing, microcapillary needle arrangements<sup>42</sup>. **c** | Complex 3D structures fabricated using membrane-assisted photolithography, which facilitates sequential, layered polymerizations. The confocal microscopy image shows the cross section of the particle, the inset its 3D morphology<sup>56</sup>. Panel **a** is adapted from reF.<sup>123</sup>, panel **b** from reF.<sup>42</sup>, panel **c** from reF.<sup>56</sup>.

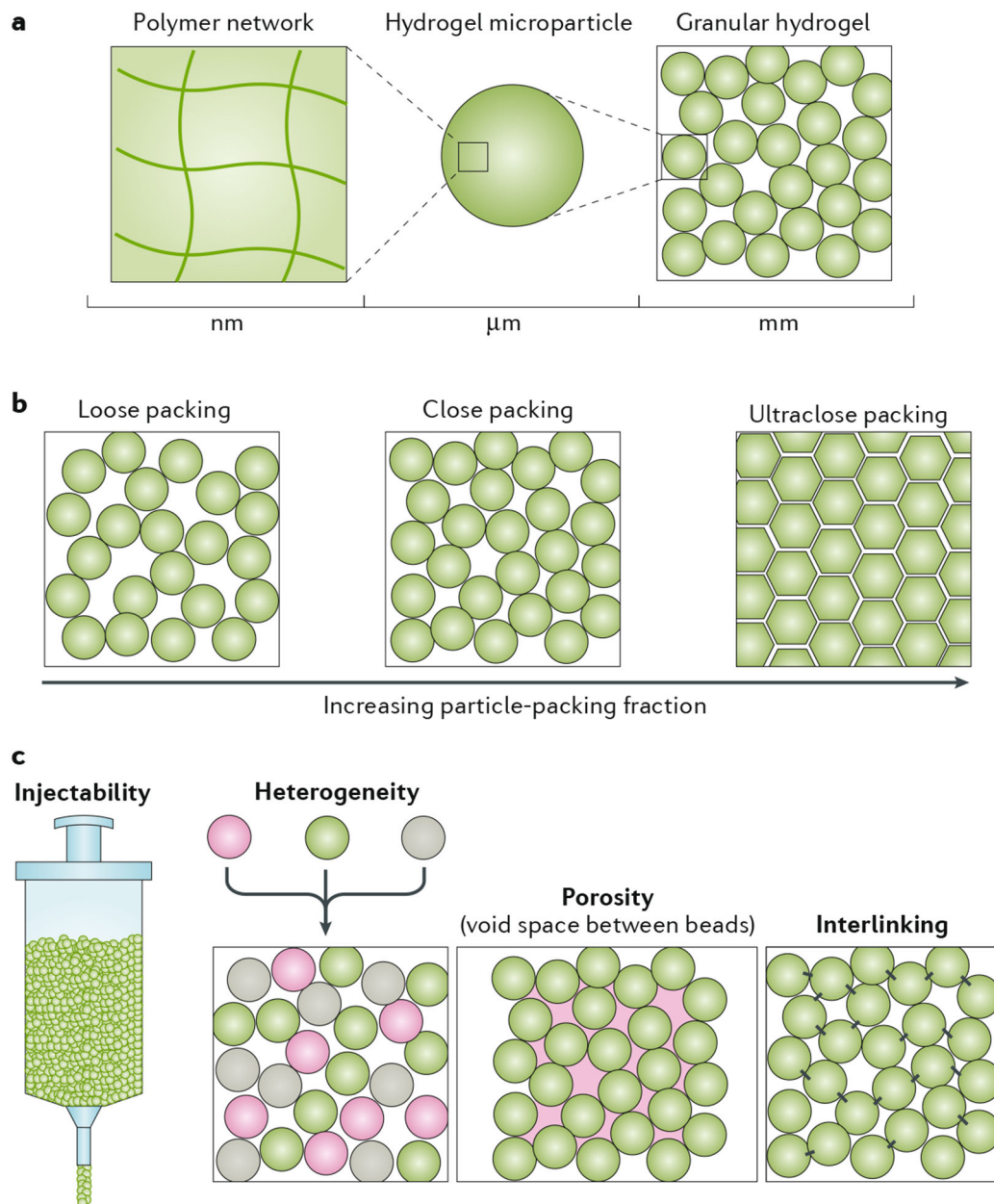


**Fig. 4 | Structure and properties of granular hydrogels.**

**a** | Granular hydrogels have multiscale features, with the polymer network at the nanoscale, individual hydrogel microparticles (HMPs) at the microscale and the granular structure at the millimetre scale. **b** | When the particle-packing fraction of HMPs in a granular hydrogel increases, the system evolves from loose packing to close packing to, eventually, an ultraclose-packing state, in which the particles deform and void spaces collapse. The packing density affects physical properties such as porosity, transport and mechanical properties. **c** | Granular hydrogels have unique features, including injectability, heterogeneity (if different types of HMPs are mixed together) and porosity, which allows for passage through the structure. Interlinking between particles further stabilizes the structure.

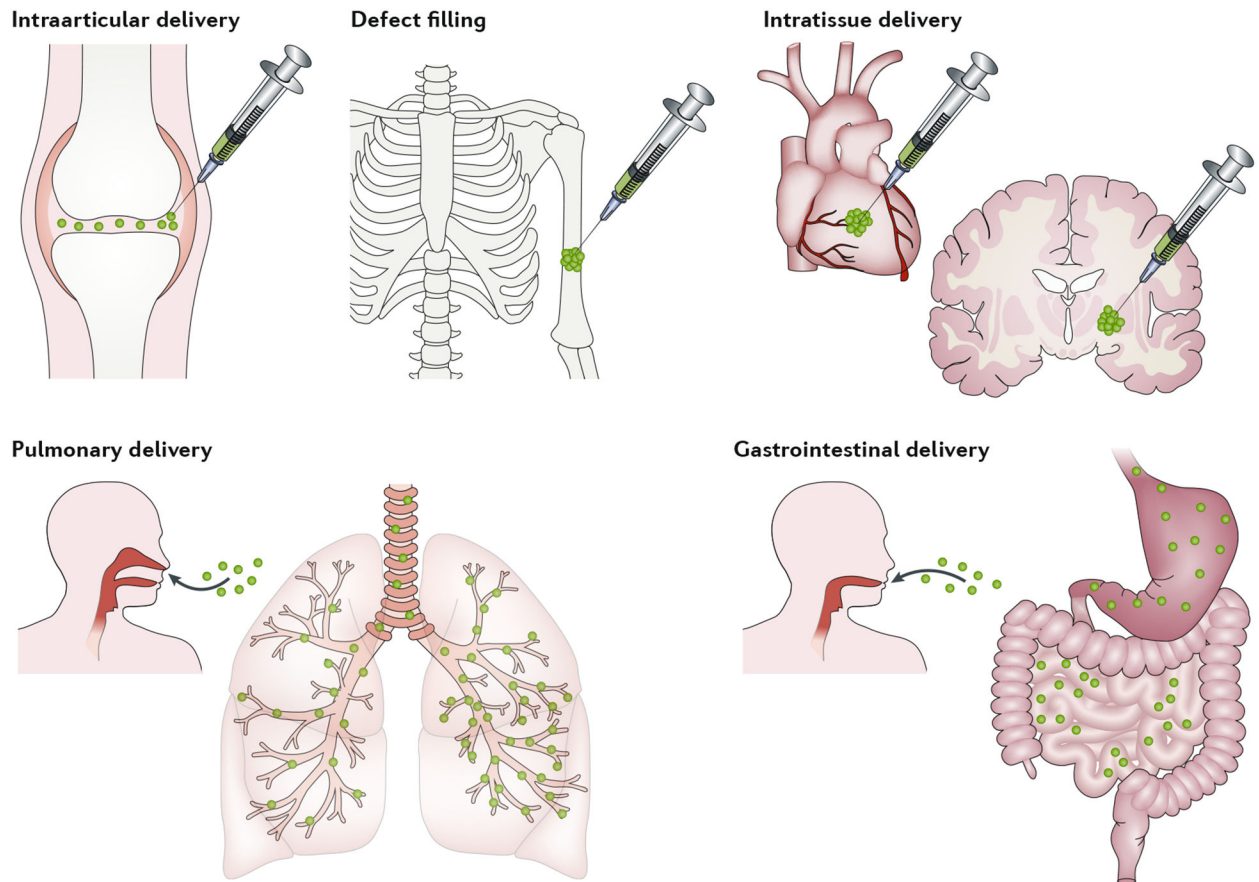


**Fig. 5 | Hydrogel microparticles delivery to various tissues in the body.**

Examples of hydrogel microparticle delivery include: delivery to the intraarticular space; delivery to bone defects; intratissue delivery (for example, in the heart or brain); delivery to the lungs via aerosols; and delivery through the gastrointestinal tract to the intestine. Hydrogel microparticles can be delivered as suspensions, granular hydrogels or composites, and they may contain biologics, such as cells or drugs.



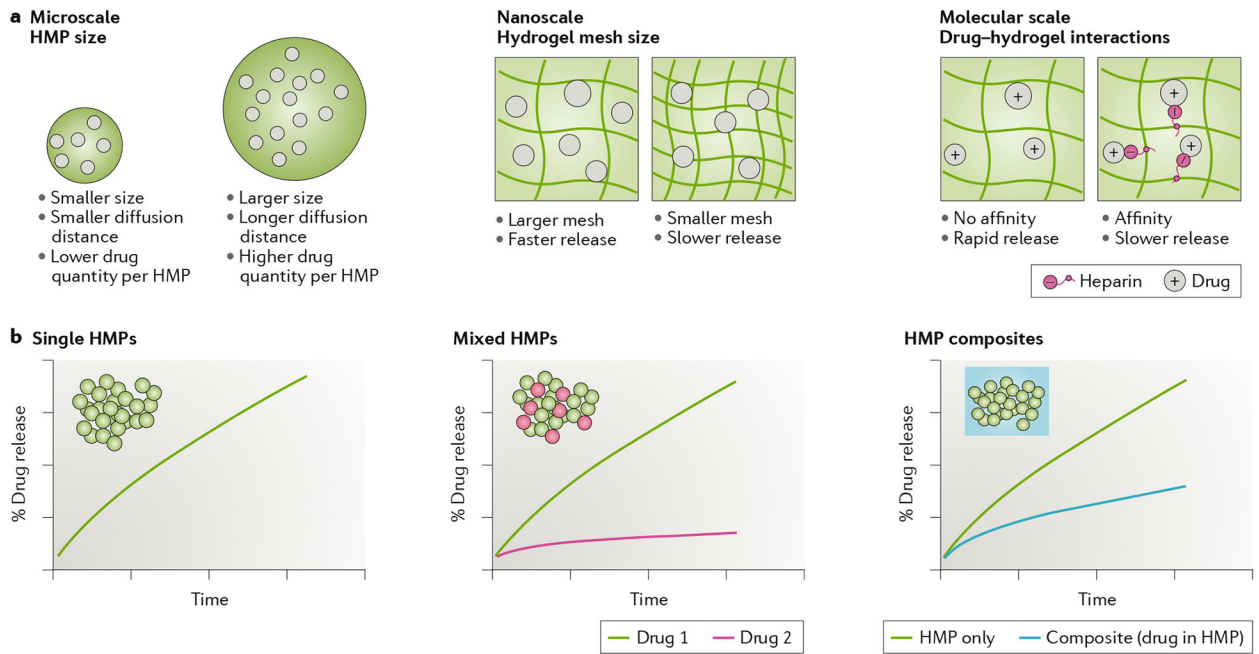


**Fig. 6 | Drug release from hydrogel microparticles.**

**a** | General parameters that influence drug release from hydrogel microparticles (HMPs) are the particle size, network mesh size and molecular interactions between drug and hydrogel.

**b** | Potential release profiles of drugs from HMPs for single HMP formulations, mixed HMP formulations to deliver multiple drugs and composites in which HMPs are embedded within a bulk hydrogel.

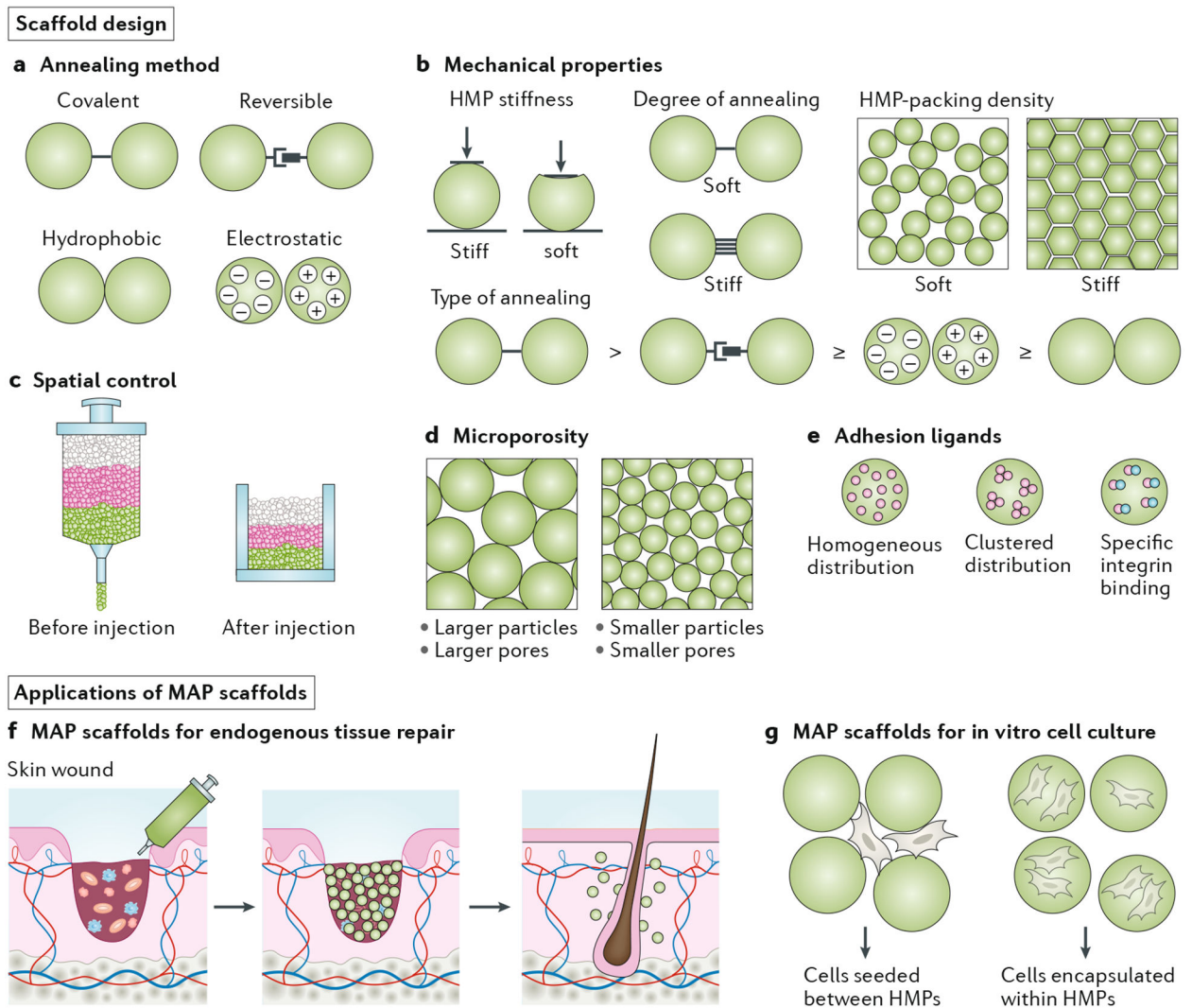


**Fig. 7 | Design considerations for building scaffolds from hydrogel microparticles.**

Scaffold design includes the engineering of: **a** | The annealing chemistry (which can be covalent, reversible, electrostatic or hydrophobic, resulting in various strengths of interactions) used to form microporous annealed particle (MAP) scaffolds. **b** | The mechanical properties, which are modulated by the stiffness of the individual hydrogel microparticles (HMPs), the degree of annealing (number of bonds between HMPs), the HMP-packing density and the chemistry of annealing (for example, covalent bonding is stronger than non-covalent bonding). **c** | Spatial control during injection. **d** | HMP size, which influences microporosity. **e** | Ligand modification for adhesion (distribution and type of ligand presentation). Applications of HMPs include: **f** | Cutaneous endogenous repair. **g** | Cell culture (intraparticle and interparticle culture platforms).

## HMP assembly

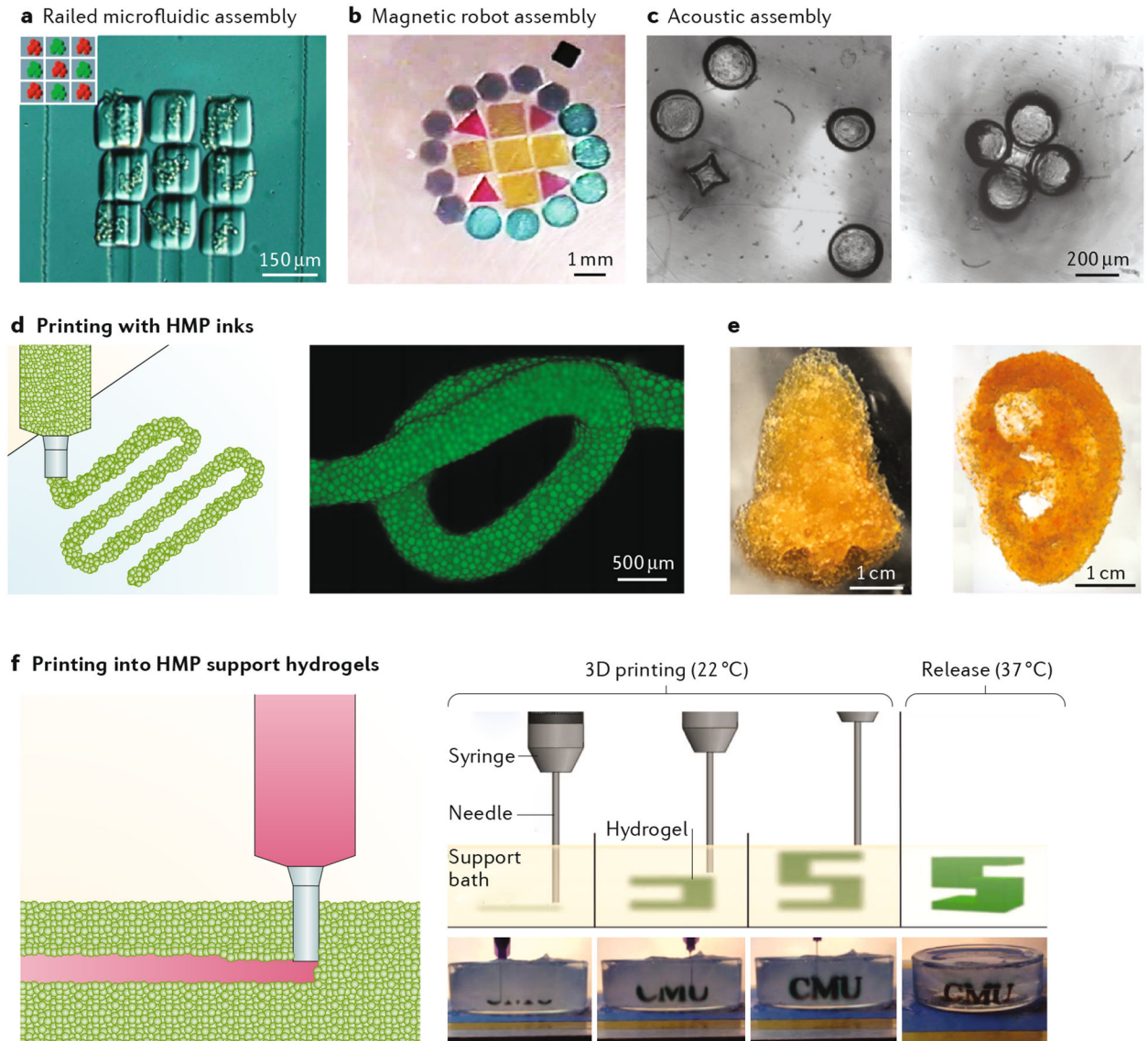


**Fig. 8 | Hydrogel microparticles in biofabrication.**

Examples of hydrogel microparticle (HMP) bioassembly approaches, which include: **a** | Railed microfluidic bioassembly, in which cell-containing poly(ethylene glycol) diacrylate HMPs are fluidically guided along complementarily grooved microchannels<sup>57</sup>. **b** | Magnetically guided bioassembly of poly(ethylene glycol) diacrylate HMPs into 2D structures using untethered microrobots<sup>214</sup>. **c** | Acoustically guided bioassembly of complimentary shaped HMPs<sup>215</sup>. **d** | Extrusion printing of jammed-particle ink filaments prepared using hyaluronic-acid HMPs<sup>7</sup>. **e** | Ear-shaped and nose-shaped structures printed using jammed poly(ethylene glycol) HMPs<sup>217</sup>. **f** | Schematic illustrating the printing of a hydrogel ink into a HMP-based support medium, accompanied by an example of this approach, in which gelatin HMPs were used as a thermoreversible support bath in which the hydrogel precursor ink was deposited to form the letters CMU<sup>86</sup>. Panel **a** is adapted from

reF.<sup>57</sup>, panel **b** from reF.<sup>214</sup>, panel **c** from reF.<sup>215</sup>, panel **d** from reF.<sup>7</sup>, panel **e** from reF.<sup>217</sup>, panel **f** from reF.<sup>86</sup>.

Author Manuscript

Author Manuscript

Author Manuscript

Author Manuscript

**Table 1 |** Key performance metrics for different techniques for the fabrication of hydrogel microparticles

Production method	Particle size coefficient of variation* (CV%)	Minimum size range	Production rate	Particle geometry	Compatibility with cells
Batch emulsion	Large variation (>10%) <sup>1,2,30</sup>	1–10 $\mu\text{m}$ <sup>17</sup>	High (only limited by vessel size)	Spherical	Average (>80% viability) <sup>11,12</sup>
Microfluidic emulsion	Low variation (1–2% possible) <sup>2,6</sup>	5–10 $\mu\text{m}$ <sup>4,23,4,51</sup>	Average (can be improved with parallel channels)	Spherical	Average (>80% viability) <sup>33,38,47</sup>
Lithography	Low variation (1–3% possible) <sup>6,1,75,231</sup>	<1 $\mu\text{m}$ possible <sup>6,1,62</sup>	Low (can be improved when integrated with microfluidics)	Arbitrary 2D and 3D geometries possible	High (>90%); no oil or surfactant required <sup>38,59</sup>
Electrohydrodynamic spraying	Average variation >50% <sup>77,79,80</sup>	1–10 $\mu\text{m}$ <sup>78</sup>	Average	Spherical	Average (>80%) <sup>76,77</sup>
Mechanical fragmentation	Average variation (2–8%) <sup>86</sup>	20–50 $\mu\text{m}$ <sup>85,86</sup>	High (only limited by vessel size)	Irregular	Unreported

\* The coefficient of variation (CV%) is defined as the ratio of the standard deviation of particle size to the mean particle size.

Table 2 |

Hydrogel cross-linking chemistries used to generate hydrogel microparticles

Base hydrogel	Chemical modification	Cross-linking method	Fabrication technique
Alginate	Unmodified <sup>77</sup>	Ionic cross-linking with CaCl <sub>2</sub>	EHD spraying
	Unmodified <sup>47,112</sup>	Ionic cross-linking in the presence of CaCl <sub>2</sub>	Microfluidic emulsion
	Methacrylate <sup>232</sup>	Radical polymerization (UV)	Microfluidic emulsion
Gelatin	Unmodified <sup>86</sup>	Temperature	Mechanical fragmentation
	Methacrylate <sup>35,233</sup>	Radical polymerization (UV)	Microfluidic emulsion
	Methacrylate <sup>194</sup>	Temperature (cooling to 4 °C then radical polymerization (UV))	Microfluidic emulsion
Methacrylate <sup>58</sup>	Radical polymerization (UV)	Lithography	
	Methacrylate <sup>234</sup>	Radical polymerization (UV)	Batch emulsion
	Methacrylate <sup>67</sup>	Radical polymerization (UV)	Lithography
Acrylate <sup>103</sup>	Radical polymerization (UV)	Microfluidic emulsion	
	Norbornene <sup>7</sup>	Thiol-ene reaction	Microfluidic emulsion
	Tyramine <sup>235</sup>	Sequential enzymatic and radical polymerization (UV)	Lithography (two-photon)
Tyramine + furan <sup>236</sup>	Enzymatic cross-linking and/or Diels–Alder click chemistry	Microfluidic emulsion	
	Vinyl ester <sup>69</sup>	Thiol-ene reaction	Lithography (two-photon)
	Aldehyde + hydrazide <sup>237</sup>	Hydrazone covalent cross-linking	Batch emulsion
Methacrylate + tetrazole <sup>238</sup>	Tetrazole–alkene photoclick chemistry (UV)	Microfluidic emulsion	
	Acrylate <sup>59,239,240</sup>	Radical polymerization (UV)	Microfluidic emulsion and lithography
	Methacrylate <sup>34</sup>	Radical polymerization (UV)	Lithography
Norbornene <sup>95</sup>	Thiol-ene reaction (UV)	EHD spraying	
	Vinyl sulfone <sup>8</sup>	Michael addition	Microfluidic emulsion
	Vinyl sulfone and thiol <sup>39,125</sup>	Michael addition	Microfluidic emulsion
Maleimide <sup>29,33,38</sup>	Michael addition	Microfluidic emulsion	
	Thiol and ene <sup>68</sup>	Thiol-ene reaction (UV)	Lithography
	Unmodified <sup>82</sup>	Electrostatic interactions	EHD spraying
Silk/fibroin	Norbornene <sup>241</sup>	Thiol-ene photoclick chemistry and $\beta$ -sheet formation	Batch emulsion



Base hydrogel	Chemical modification	Cross-linking method	Fabrication technique
Agarose	Unmodified <sup>7,37,42</sup>	Temperature	Microfluidic emulsion

EDH, electrohydrodynamic; PEG, poly(ethylene glycol); PVA, poly(vinyl alcohol); UV, ultraviolet.

Author Manuscript

Author Manuscript

Author Manuscript

Author Manuscript